role in this syndrome (OMIM 180860). We first identified SNPs in the previously reported 22 human DMRs using genomic DNA isolated from human sperm and blood from unaffected individuals, which could then be used in bisulfite-PCR methylation assays to assign methylation to the parental allele. We next collected a total of 15 SRS samples, including previously collected samples (ART: 2, naturally conceived: 4), which had DNA methylation errors at the paternal gDMR at *H19*. Five of these were born from ART and 10 were from natural conceptions. We analyzed and compared the DNA methylation status of the 3 other paternal gDMRs and the 19 maternal gDMRs (Supplementary data, Fig. S3, Table, Supplementary data, Table SIV). In four out of the five ART cases, DNA methylation errors were not restricted to the *H19* gDMR, and were present at both maternally and paternally methylated gDMRs. These four cases showed a mixture of hyper- and hypomethylation with mosaic (partial) patterns. In contrast, only 3 of the 10 naturally conceived patients showed DNA methylation errors at loci other than *H19* gDMR.

To determine whether DNA methylation errors occurred in patients at a broader level in the genomes, we assessed the methylation profiles of the non-imprinted *LINE1* and *Alu* elements. We examined a total of 28 CpG sites in a 413-bp fragment of *LINE1* and 12 CpG sites in a 152-bp fragment of *Alu* (Supplementary data, Table SIV), and no significant differences were found in the methylation ratios between patients conceived by ART and naturally.

The abnormal methylation pattern in BWS patients with epimutations

In BWS, hypermethylation of *H19* or hypomethylation of *KCNQ1OT1(LIT1)* at human chromosome 11 are both frequently reported (Choufani *et al.*, 2010). We collected seven BWS samples with DNA methylation errors of the *LIT1* gDMR, one of which was derived from ART patient and six from naturally conceived patients (Supplementary data, Fig. S3, Table II, Supplementary data, Table SIV). In the one ART (ICSI) case, we identified four additionally gDMR methylation errors, again present at both maternally and paternally methylated gDMRs and with mixed hyper- and hypomethylation patterns. Furthermore, the methylation error at the *NESPAS* DMR was mosaic in this patient. One of the six naturally BWS cases had similar changes. Although we had only one BWS case conceived by ART, widespread methylation errors were similar to those for the DNA methylation error pattern in SRS.

Phenotypic differences between ART patients and those conceived naturally

The increased frequency of DNA methylation errors at other loci in the ART cases suggested that the BWS and SRS cases born after ART might exhibit additional phenotypic characteristics. However, when we compared in detail the clinical features from both categories of conception (Supplementary data, Table SV), we found no major differences between ART and naturally conceived patients with BWS and SRS.

Discussion

Our key finding from this study was a possible association between ART and the imprinting disorders, BWS and SRS. We did not find a similar association with PWS and AS but our numbers were quite low in this study and a larger due to the questionnaire return rate and relative rarity of the diseases, international study will be required to reach definitive conclusions. Furthermore, factors such as PCR and/or cloning bias in the bisulfite method and correction for changing rate of ART over time must be considered when analyzing any results.

In addition to the possible association between ART and BWS/SRS, we observed a more widespread disruption of genomic imprints after ART. The increased frequency of imprinting disorders after ART shown by us and others is perhaps not surprising given the major epigenetic events that take place during early development at a time when the epigenome is most vulnerable. The process of ART exposes the developing epigenome to many external influences, which have been shown to influence the proper establishment and maintenance of genomic imprints, including hormone stimulation (Sato *et al.*, 2007), *in vitro* culturing (DeBaun *et al.*, 2003; Gicquel *et al.*, 2003; Maher *et al.*, 2003), cryopreservation (Emiliani *et al.*, 2000; Honda *et al.*, 2001) and the timing of embryo transfer (Shimizu *et al.*, 2004; Miura and Niikawa, 2005). Furthermore, we and others have also shown that some infertile males, particularly those with oligozoospermia, carry pre-existing imprinting errors in their sperm (Marques *et al.*, 2004; Kobayashi *et al.*, 2007; Marques *et al.*, 2008) which might account for the association between ART and imprinting disorders.

Imprinting syndromes and their association with ART

We report the first Japanese nationwide epidemiological study to examine four well-known imprinting diseases and their possible association with ART. We found that the frequency of ART use in both BWS and SRS was higher than anticipated based on the nationwide frequency of ART use at the time when these patients were born. Several other reports have raised concerns that children conceived by ART have an increased risk of disorders (Cox *et al.*, 2002; DeBaun *et al.*, 2003; Maher *et al.*, 2003; Orstavik *et al.*, 2003; Ludwig *et al.*, 2005; Lim and Maher, 2009). However, the association is not clear in every study (Lidegaard *et al.*, 2005; Doornbos *et al.*, 2007). The studies reporting an association were mainly from case reports or case series whereas the studies where no association was reported were cohort studies. Therefore, the differences in the epidemiological analytical methods might accounts for the disparity in findings.

Owing to the rare nature of the imprinting syndromes, statistical analysis is challenging. In addition, the diagnosis of imprinting diseases is not always clear cut. Many of the syndromes have a broad clinical spectrum, different molecular pathogenesis, and the infant has to have reached a certain age before these diseases become clinically detectable. It is therefore likely that some children with these diseases are not recorded with the specific diagnosis code for these syndromes. Nonetheless, in this study we were examining the relationship between ART and the imprinting syndromes and these confounding factors are likely to apply equally to both groups.

Both BWS and SRS occurred after ART but our numbers for PWS and AS were low, precluding any definitive conclusion for these two disorders. However, while most cases of BWS and SRS are caused by an epimutation, epimutations are very rare in PWS and AS (only 1–4%) and ART would not be expected to increase chromosome 15

Table II Abnormal methylation in patients with SRS and BWS.

Case	ART	Abnormal methylation			
SRS					
SRS-1	IVF-ET	H19 hypomethylated (mosaic)	PEG1 hypermethylated	PEG10 hypermethylated (mosaic)	GRB10 hypermethylated; ZNF597 hypomethylated
SRS-2	IVF-ET	H19 hypomethylated (mosaic)			
SRS-3	IVF-ET	H19 hypomethylated (mosaic)	PEG1 hypermethylated (mosaic)		
SRS-4	IVF-ET	H19 hypomethylated	GRB10 hypermethylated		
SRS-5	IVF-ET	H19 hypomethylated (mosaic)	INPP5F hypermethylated		
SRS-6		H19 hypomethylated			
SRS-7		H19 hypomethylated (mosaic)	ZNF597 hypermethylated (mosaic)	ZNF331 hypomethylated (mosaic)	
SRS-8		H19 hypomethylated			
SRS-9		H19 hypomethylated (mosaic)			
SRS-10		H19 hypomethylated			
SRS-11		H19 hypomethylated (mosaic)	PEG1 hypermethylated		
SRS-12		H19 hypomethylated			
SRS-13		H19 hypomethylated (mosaic)	FAM50B hypomethylated		
SRS-14		H19 hypomethylated			
SRS-15		H19 hypomethylated			
BWS					
BWS-1	ICSI	LIT1 hypomethylated	ZDBF2 hypermethylated	PEG1 hypermethylated	NESPAS hypomethylated (mosaic)
BWS-2		LIT1 hypomethylated			
BWS-3		LIT1 hypomethylated			
BWS-4		LIT1 hypomethylated			
BWS-5		LIT1 hypomethylated			
BWS-6		LIT1 hypomethylated	ZDBF2 hypomethylated	ZNF331 hypomethylated (mosaic)	
BWS-7		LIT1 hypomethylated			

ET, embryo transfer. Summary of the abnormal methylation patterns in the ART conceived and naturally conceived patients with Silver-Russell syndrome (SRS) and Beckwith-Wiedemann syndrome (BWS) with epimutations. Numbers in parentheses show the results of the methylation rates obtained using bisulfite-PCR sequencing. The % of DNA methylation of 22 gDMRs in all patients with SRS and BWS examined are presented in Supplementary data, Table SIV. Depictions in red represent DMRs normally exclusively methylated on the maternal allele, while blue represent paternally methylated sites.

deletions or uniparental disomy, consistent with our findings. Prior to this investigation, there was some evidence for an increased prevalence of BWS after ART but less evidence for an increased prevalence of SRS, with five SRS patients reported linked to ART (Svensson *et al.*, 2005; Bliek *et al.*, 2006; Kagami *et al.*, 2007; Galli-Tsinopoulou *et al.*, 2008). Our population-wide study provides evidence to suggest that both BWS and SRS occur more frequently after ART in the Japanese population.

Mechanisms of epimutation in the patients conceived by ART

By performing a comprehensive survey of all the known gDMRs in a number of patients with BWS and SRS, we found that multiple loci were more likely to be affected in ART cases than those conceived naturally. Lim *et al.* (2009) have reported a similarly increased frequency of multiple errors after ART, with 37.5% of patients conceived with ART and 6.4% of naturally conceived patients displaying abnormal methylation at additional imprinted loci. However, while Bliek *et al.* (2009) reported alterations in multiple imprinted loci in 17 patients out of 81 BWS cases with hypomethylation of *KCNQ1OT1*(*LIT1*) ICR, only 1 of the cases with multiple alterations was born after ART. Similarly, Rossignol *et al.* (2006) reported that 3 of 11 (27%) ART-conceived patients and 7 of 29 (24%) naturally conceived patients displayed abnormal methylation at additional loci. In these four earlier studies, not all gDMRs were assayed and it may be that by doing so, these incongruities will be resolved.

The pattern of cellular mosaicism we observed in some patients suggested that the imprinting defects occurred after fertilization rather than in the gamete as DNA methylation alterations arising in the gamete would be anticipated to be present in every somatic cell. This suggested the possibility that the DNA methylation errors occurred as a consequence of impaired maintenance of the germline imprints rather than a failure to establish these imprints in the germline or a loss of these imprints in the sperm or oocytes *in vitro*. Furthermore, some patients conceived by ART with SRS and BWS showed

alterations at both maternally and paternally methylated gDMRs suggesting that the defects were not limited to one parental germline. The mechanisms controlling the protection of imprinted loci against demethylation early in the development remain unclear. Our data suggested that this protection may fail in ART resulting in the tissue-specific loss of imprints, though it remains unclear if this ever occurs naturally. Potential factors involved could include the culture conditions for the newly fertilized oocyte and the length of exposure to specific media or growth factors, as part of the ART procedure. Some of the naturally conceived patients also had abnormal methylation at both maternally and paternally methylated gDMRs, which were in some cases mosaic. This could indicate that fertility issues arise as a consequence of pre-existing mutations in factors required to protect and maintain imprints early in life and it may therefore be possible to identify genetic mutations in these factors in this group of patients.

Clinical features

In our large-scale epidemiological study, we found differences in the frequency of some classic features of SRS and BWS between patients conceived by ART and those conceived naturally. We found that 7/7 (100%) ART conceived SRS patients showed body asymmetry, whereas only 30/54 (55.5%) who were conceived naturally possessed this feature. Similarly in BWS, earlobe creases were present in 4/7 (57.1%) ART conceived cases and 44/89 (49.4%) naturally conceived, bulging eyes in 3/7 (42.8%) versus 21/89 (23.6%), exomphalos in 6/7 (85.7%) versus 61/89 (68.5%) and nephromegaly in 2/7 (28.6%) versus 18/89 (20.2%), respectively. It is therefore possible that the dysregulation of the additional genes does modify the typical SRS and BWS phenotypes (Azzi *et al.*, 2010). BWS patients with multiple hypermethylation sites have been reported with complex clinical phenotypes (Bliek *et al.*, 2009) and a recently recognized BWS-like syndrome involving overgrowth with severe developmental delay was reported after IVF/ICSI (Shah *et al.*, 2006).

In our study patients with diagnosed imprinting disorders that presented with defects at additional loci (i.e. other than the domain responsible for that disorder) did not display additional phenotypes not normally reported in BWS or SRS. Since we were effectively selecting for classic cases of BWS and SRS in the first instance, it is possible that there are individuals born through ART showing entirely novel or confounding phenotypes that were not identified in our survey. Alternatively, as many of the alterations we observed showed a mosaic pattern, it is possible that mosaic individuals have more subtle phenotypes. In light of this new information on mosaicism, we may be able to use our knowledge of the individual's epigenotype to uncover these subtle changes.

This study, and the work of our colleagues, highlights the pressing need to conduct long-term international studies on ART treatment and the prevalence of imprinting disorders, particularly as the use of ART is increasing worldwide. It remains to be seen if other very rare epigenetic disorders will also have a possible association with the use of ART. Furthermore, it is not yet known what other pathologies might be influenced by ART. For example, in addition to general growth abnormalities, many imprint methylation errors also lead to the occurrence of various cancers (Okamoto *et al.*, 1997; Cui *et al.*, 1998). Further molecular studies will be required to understand the pathogenesis of these associations, and also to identify preventative methods to reduce the risk of occurrence of these syndromes following ART.

Supplementary data

Supplementary data are available at http://humrep.oxfordjournals.org/.

Acknowledgements

The authors thank the patients and their families who participated in this study. We are also grateful to the physicians who responded to the first and second surveys. We would like to thank Ms Chizuru Abe for technical assistance.

Authors' roles

H.H., H.O., N.M., F.S. and A.S. performed the DNA methylation analyses. M.K., K.N. and H.S. collected the samples of the patients. K.N. did the statistical analyses. H.H., M.V.D.P., R.M.J. and T.A. wrote this manuscript. All authors have read and approved the final manuscript.

Funding

This work was supported by Grants-in-Aid from the Ministry of Health, Labour and Welfare of the Japanese government (The Specified Disease Treatment Research Program; 162, 054) and Scientific Research (KAKENHI; 21028003, 23013003, 23390385), as well as the Uehara Memorial Foundation and Takeda Science Foundation (TA).

Conflict of interest

None declared.

References

Azzi S, Rossignol S, Le Bouc Y, Netchine I. Lessons from imprinted multilocus loss of methylation in human syndromes: A step toward understanding the mechanisms underlying these complex diseases. *Epigenetics* 2010;**5**:373–377.

Bliek J, Terhal P, van den Bogaard MJ, Maas S, Hamel B, Salieb-Beugelaar G, Simon M, Letteboer T, van der Smagt J, Kroes H *et al.* Hypomethylation of the H19 gene causes not only Silver-Russell syndrome (SRS) but also isolated asymmetry or an SRS-like phenotype. *Am J Hum Genet* 2006;**78**:604–614.

Bliek J, Verde G, Callaway J, Maas SM, De Crescenzo A, Sparago A, Cerrato F, Russo S, Ferraiuolo S, Rinaldi MM *et al.* Hypomethylation at multiple maternally methylated imprinted regions including PLAGL1 and GNAS loci in Beckwith-Wiedemann syndrome. *Eur J Hum Genet* 2009;**17**:611–619.

Bowdin S, Allen C, Kirby G, Brueton L, Afnan M, Barratt C, Kirkman-Brown J, Harrison R, Maher ER, Reardon W. A survey of assisted reproductive technology births and imprinting disorders. *Hum Reprod* 2007;**22**:3237–3240.

Chang AS, Moley KH, Wangler M, Feinberg AP, Debaun MR. Association between Beckwith-Wiedemann syndrome and assisted reproductive technology: a case series of 19 patients. *Fertil Steril* 2005;**83**:349–354.

Choufani S, Shuman C, Weksberg R. Beckwith-Wiedemann syndrome. *Am J Med Genet Part C Semin Med Genet* 2010;**154C**:343–354.

Cox GF, Burger J, Lip V, Mau UA, Sperling K, Wu BL, Horsthemke B. Intracytoplasmic sperm injection may increase the risk of imprinting defects. *Am J Hum Genet* 2002;**71**:162–164.

Cui H, Horon IL, Ohlsson R, Hamilton SR, Feinberg AP. Loss of imprinting in normal tissue of colorectal cancer patients with microsatellite instability. *Nat Med* 1998;**4**:1276–1280.

DeBaun MR, Niemitz EL, Feinberg AP. Association of in vitro fertilization with Beckwith-Wiedemann syndrome and epigenetic alterations of LIT1 and H19. *Am J Hum Genet* 2003;**72**:156–160.

Doornbos ME, Maas SM, McDonnell J, Vermeiden JP, Hennekam RC. Infertility, assisted reproduction technologies and imprinting disturbances: a Dutch study. *Hum Reprod* 2007;**22**:2476–2480.

Emiliani S, Van den Bergh M, Vannin AS, Biramane J, Englert Y. Comparison of ethylene glycol, 1,2-propanediol and glycerol for cryopreservation of slow-cooled mouse zygotes, 4-cell embryos and blastocysts. *Hum Reprod* 2000;**15**:905–910.

Galli-Tsinopoulou A, Emmanouilidou E, Karagianni P, Grigoriadou M, Kirkos J, Varlamis GS. A female infant with Silver Russell syndrome, mesocardia and enlargement of the clitoris. *Hormones (Athens)* 2008; **7**:77–81.

Gicquel C, Gaston V, Mandelbaum J, Siffroi JP, Flahault A, Le Bouc Y. In vitro fertilization may increase the risk of Beckwith-Wiedemann syndrome related to the abnormal imprinting of the KCN1OT gene. *Am J Hum Genet* 2003;**72**:1338–1341.

Gosden R, Trasler J, Lucifero D, Faddy M. Rare congenital disorders, imprinted genes, and assisted reproductive technology. *Lancet* 2003; **361**:1975–1977.

Honda S, Weigel A, Hjelmeland LM, Handa JT. Induction of telomere shortening and replicative senescence by cryopreservation. *Biochem Biophys Res Commun* 2001;**282**:493–498.

John RM, Lefebvre L. Developmental regulation of somatic imprints. *Differentiation* 2011;**81**:270–280.

Kagami M, Nagai T, Fukami M, Yamazawa K, Ogata T. Silver-Russell syndrome in a girl born after in vitro fertilization: partial hypermethylation at the differentially methylated region of PEG1/ MEST. *J Assist Reprod Genet* 2007;**24**:131–136.

Kikyo N, Williamson CM, John RM, Barton SC, Beechey CV, Ball ST, Cattanach BM, Surani MA, Peters J. Genetic and functional analysis of neuronatin in mice with maternal or paternal duplication of distal Chr 2. *Dev Biol* 1997;**190**:66–77.

Kobayashi H, Suda C, Abe T, Kohara Y, Ikemura T, Sasaki H. Bisulfite sequencing and dinucleotide content analysis of 15 imprinted mouse differentially methylated regions (DMRs): paternally methylated DMRs contain less CpGs than maternally methylated DMRs. *Cytogenet Genome Res* 2006;**113**:130–137.

Kobayashi H, Sato A, Otsu E, Hiura H, Tomatsu C, Utsunomiya T, Sasaki H, Yaegashi N, Arima T. Aberrant DNA methylation of imprinted loci in sperm from oligospermic patients. *Hum Mol Genet* 2007;**16**:2542–2551.

Kobayashi H, Yamada K, Morita S, Hiura H, Fukuda A, Kagami M, Ogata T, Hata K, Sotomaru Y, Kono T. Identification of the mouse paternally expressed imprinted gene Zdbf2 on chromosome 1 and its imprinted human homolog ZDBF2 on chromosome 2. *Genomics* 2009; **93**:461–472.

Lidegaard O, Pinborg A, Andersen AN. Imprinting diseases and IVF: Danish National IVF cohort study. *Hum Reprod* 2005;**20**:950–954.

Lim D, Bowdin SC, Tee L, Kirby GA, Blair E, Fryer A, Lam W, Oley C, Cole T, Brueton LA *et al.* Clinical and molecular genetic features of Beckwith-Wiedemann syndrome associated with assisted reproductive technologies. *Hum Reprod* 2009;**24**:741–747.

Lim DH, Maher ER. Human imprinting syndromes. *Epigenomics* 2009; **1**:347–369.

Lucifero D, Mertineit C, Clarke HJ, Bestor TH, Trasler JM. Methylation dynamics of imprinted genes in mouse germ cells. *Genomics* 2002; **79**:530–538.

Ludwig M, Katalinic A, Gross S, Sutcliffe A, Varon R, Horsthemke B. Increased prevalence of imprinting defects in patients with Angelman syndrome born to subfertile couples. *J Med Genet* 2005;**42**:289–291.

Maher ER, Brueton LA, Bowdin SC, Luharia A, Cooper W, Cole TR, Macdonald F, Sampson JR, Barratt CL, Reik W *et al.* Beckwith-Wiedemann syndrome and assisted reproduction technology (ART). *J Med Genet* 2003;**40**:62–64.

Marques CJ, Carvalho F, Sousa M, Barros A. Genomic imprinting in disruptive spermatogenesis. *Lancet* 2004;**363**:1700–1702.

Marques CJ, Costa P, Vaz B, Carvalho F, Fernandes S, Barros A, Sousa M. Abnormal methylation of imprinted genes in human sperm is associated with oligozoospermia. *Mol Hum Reprod* 2008;**14**:67–74.

Miura K, Niikawa N. Do monochorionic dizygotic twins increase after pregnancy by assisted reproductive technology? *J Hum Genet* 2005; **50**:1–6.

Moll AC, Imhof SM, Cruysberg JR, Schouten-van Meeteren AY, Boers M, van Leeuwen FE. Incidence of retinoblastoma in children born after in-vitro fertilisation. *Lancet* 2003;**361**:309–310.

Obata Y, Kono T. Maternal primary imprinting is established at a specific time for each gene throughout oocyte growth. *J Biol Chem* 2002; **277**:5285–5289.

Okamoto K, Morison IM, Taniguchi T, Reeve AE. Epigenetic changes at the insulin-like growth factor II/H19 locus in developing kidney is an early event in Wilms tumorigenesis. *Proc Natl Acad Sci USA* 1997; **94**:5367–5371.

Orstavik KH, Eiklid K, van der Hagen CB, Spetalen S, Kierulf K, Skjeldal O, Buiting K. Another case of imprinting defect in a girl with Angelman syndrome who was conceived by intracytoplasmic semen injection. *Am J Hum Genet* 2003;**72**:218–219.

Rossignol S, Steunou V, Chalas C, Kerjean A, Rigolet M, Viegas-Pequignot E, Jouannet P, Le Bouc Y, Gicquel C. The epigenetic imprinting defect of patients with Beckwith-Wiedemann syndrome born after assisted reproductive technology is not restricted to the 11p15 region. *J Med Genet* 2006;**43**:902–907.

Sato A, Otsu E, Negishi H, Utsunomiya T, Arima T. Aberrant DNA methylation of imprinted loci in superovulated oocytes. *Hum Reprod* 2007;**22**:26–35.

Savage T, Peek J, Hofman PL, Cutfield WS. Childhood outcomes of assisted reproductive technology. *Hum Reprod* 2011;**26**:2392–2400.

Shah PS, Weksberg R, Chitayat D. Overgrowth with severe developmental delay following IVF/ICSI: a newly recognized syndrome? *Am J Med Genet A* 2006;**140**:1312–1315.

Shimizu Y, Fukuda J, Sato W, Kumagai J, Hirano H, Tanaka T. First-trimester diagnosis of conjoined twins after in-vitro fertilization-embryo transfer (IVF-ET) at blastocyst stage. *Ultrasound Obstet Gynecol* 2004;**24**:208–209.

Smith RJ, Dean W, Konfortova G, Kelsey G. Identification of novel imprinted genes in a genome-wide screen for maternal methylation. *Genome Res* 2003;**13**:558–569.

Surani MA. Imprinting and the initiation of gene silencing in the germ line. *Cell* 1998;**93**:309–312.

Svensson J, Bjornstahl A, Ivarsson SA. Increased risk of Silver-Russell syndrome after in vitro fertilization? *Acta Paediatr* 2005;**94**:1163–1165.

Tomizawa S, Kobayashi H, Watanabe T, Andrews S, Hata K, Kelsey G, Sasaki H. Dynamic stage-specific changes in imprinted differentially methylated regions during early mammalian development and prevalence of non-CpG methylation in oocytes. *Development* 2011;**138**:811–820.

Wakai K, Tamakoshi A, Ikezaki K, Fukui M, Kawamura T, Aoki R, Kojima M, Lin Y, Ohno Y. Epidemiological features of moyamoya disease in Japan: findings from a nationwide survey. *Clin Neurol Neurosurg* 1997;**99**(Suppl. 2):S1–S5.

Wood AJ, Roberts RG, Monk D, Moore GE, Schulz R, Oakey RJ. A screen for retrotransposed imprinted genes reveals an association between X chromosome homology and maternal germ-line methylation. *PLoS Genet* 2007;**3**:e20.

Young LE, Fernandes K, McEvoy TG, Butterwith SC, Gutierrez CG, Carolan C, Broadbent PJ, Robinson JJ, Wilmut I, Sinclair KD. Epigenetic change in IGF2R is associated with fetal overgrowth after sheep embryo culture. *Nat Genet* 2001;**27**:153–154.

CLINICAL REPORT

AMERICAN JOURNAL OF medical genetics PART A

Aberrant Methylation of H19-DMR Acquired After Implantation Was Dissimilar in Soma Versus Placenta of Patients With Beckwith–Wiedemann Syndrome

Ken Higashimoto,[1] Kazuhiko Nakabayashi,[2] Hitomi Yatsuki,[1] Hokuto Yoshinaga,[1] Kosuke Jozaki,[1] Junichiro Okada,[3] Yoriko Watanabe,[3] Aiko Aoki,[4] Arihiro Shiozaki,[4] Shigeru Saito,[4] Kayoko Koide,[1] Tsunehiro Mukai,[5] Kenichiro Hata,[2] and Hidenobu Soejima[1]*

[1]Division of Molecular Genetics & Epigenetics, Department of Biomolecular Sciences, Faculty of Medicine, Saga University, Saga, Japan

[2]Department of Maternal–Fetal Biology, National Research Institute for Child Health and Development, Setagaya, Tokyo, Japan

[3]Department of Pediatrics, Kurume University, Kurume, Japan

[4]Department of Obstetrics and Gynecology, University of Toyama, Toyama, Japan

[5]Nishikyushu University, Kanzaki, Saga, Japan

Manuscript Received: 7 October 2011; Manuscript Accepted: 19 January 2012

Gain of methylation (GOM) at the H19-differentially methylated region (H19-DMR) is one of several causative alterations in Beckwith–Wiedemann syndrome (BWS), an imprinting-related disorder. In most patients with epigenetic changes at H19-DMR, the timing of and mechanism mediating GOM is unknown. To clarify this, we analyzed methylation at the imprinting control regions of somatic tissues and the placenta from two unrelated, naturally conceived patients with sporadic BWS. Maternal H19-DMR was abnormally and variably hypermethylated in both patients, indicating epigenetic mosaicism. Aberrant methylation levels were consistently lower in placenta than in blood and skin. Mosaic and discordant methylation strongly suggested that aberrant hypermethylation occurred after implantation, when genome-wide de novo methylation normally occurs. We expect aberrant de novo hypermethylation of H19-DMR happens to a greater extent in embryos than in placentas, as this is normally the case for de novo methylation. In addition, of 16 primary imprinted DMRs analyzed, only H19-DMR was aberrantly methylated, except for NNAT DMR in the placental chorangioma of Patient 2. To our knowledge, these are the first data suggesting when GOM of H19-DMR occurs. © 2012 Wiley Periodicals, Inc.

Key words: Beckwith–Wiedemann syndrome; H19-DMR; aberrant DNA methylation; after implantation

How to Cite this Article:
Higashimoto K, Nakabayashi K, Yatsuki H, Yoshinaga H, Jozaki K, Okada J, Watanabe Y, Aoki A, Shiozaki A, Saito S, Koide K, Mukai T, Hata K, Soejima H. 2012. Aberrant methylation of H19-DMR acquired after implantation was dissimilar in soma versus placenta of patients with Beckwith–Wiedemann syndrome.
Am J Med Genet Part A 158A:1670–1675.

INTRODUCTION

Beckwith–Wiedemann syndrome (BWS) is an imprinting-related condition characterized by macrosomia, macroglossia, and abdominal wall defects (OMIM #130650). The relevant imprinted chromosomal region in BWS, 11p15.5, consists of two independent imprinted domains, *IGF2/H19* and *CDKN1C/KCNQ1OT1*. Imprinted genes within each domain are regulated by two imprinting control regions (ICR), the H19-differentially methylated region (H19-DMR) or KvDMR1 [Weksberg et al., 2010]. Several causative alterations have been identified in patients with BWS: loss of methylation (LOM) at KvDMR1, gain of methylation (GOM) at H19-DMR, paternal uniparental disomy (UPD), *CDKN1C* mutations, and chromosomal abnormality involving 11p15 [Sasaki et al., 2007; Weksberg et al., 2010].

Additional supporting information may be found in the online version of this article.

Grant sponsor: Japan Society for the Promotion of Science; Grant number: 20590330; Grant sponsor: Ministry of Health, Labor, and Welfare; Grant sponsor: National Center for Child Health and Development.

*Correspondence to:
Hidenobu Soejima, M.D., Ph.D., Professor, Division of Molecular Genetics & Epigenetics, Department of Biomolecular Sciences, Faculty of Medicine, Saga University, 5-1-1 Nabeshima, Saga 849-8501, Japan.
E-mail: soejimah@med.saga-u.ac.jp

Article first published online in Wiley Online Library (wileyonlinelibrary.com): 10 May 2012
DOI 10.1002/ajmg.a.35335

Methylation of H19-DMR is erased in primordial germ cells (PGCs) but becomes reestablished during spermatogenesis [Li, 2002; Sasaki and Matsui, 2008]: this methylation regulates the expression of *IGF2* and *H19* by functioning as a chromatin insulator, restricting access to shared enhancers [Bell and Felsenfeld, 2000; Hark et al., 2000]. GOM on the maternal H19-DMR leads to expression of both *IGF2* alleles and silencing of both *H19* alleles. Dominant maternal transmissions of microdeletions and/or base substitutions within H19-DMR have recently been reported in a few patients of BWS with H19-DMR GOM [Demars et al., 2010]. However, when and how the GOM on the maternal H19-DMR occurs is not clear.

Here, we found epigenetic mosaicism in two BWS patients. We also found that GOM at H19-DMR was discordant in blood and skin versus placenta; specifically, methylation levels were lower in placental samples. These findings strongly suggest that aberrant methylation of H19-DMR occurred after implantation. As a result, we expect aberrant de novo methylation happens to a greater extent in embryos than in placentas.

MATERIALS AND METHODS

Patients

Two unrelated patients with sporadic BWS, Patient 1 (BWS047) and Patient 2 (bwsh21-015), were delivered by cesarean in the third trimester of pregnancy. The mothers of both patients conceived naturally. Patient 1 and Patient 2 met clinical criteria for BWS as described by Elliott et al. [1994] and Weksberg et al. [2001], respectively (Table I). The placenta of Patient 1 was large and weighed 1,065 g, but was without any pathological abnormality. The placenta of Patient 2 was also large, weighing 1,620 g, and had an encapsulated placental chorangioma, as reported previously [Aoki et al., 2011]. The standard G-banding chromosome analysis using peripheral blood samples showed no abnormalities in either patient. This study was approved by the Ethics Committee for Human Genome and Gene Analyses of the Faculty of Medicine, Saga University.

Southern Blot Analysis

Genomic DNA was extracted from embryo-derived somatic tissues and the placentas of the patients (Fig. 1). Methylation-sensitive Southern blots with *Bam*HI and *Not*I were employed for KvDMR1, and blots with *Pst*I and *Mlu*I were employed for H19-DMR, as described previously [Soejima et al., 2004]. Band intensity was measured using the FLA-7000 fluoro-image analyzer (Fujifilm, Tokyo, Japan). The methylation index (MI, %) was then calculated (Fig. 1). Southern blots with *Apa*I were used to identify the microdeletion of H19-DMR as described previously [Sparago et al., 2004].

Bisulfite Sequencing and Combined Bisulfite Restriction Analysis (COBRA)

Bisulfite sequencing covering the sixth CTCF binding site (CTS6) was performed. For COBRA, PCR products of each primary imprinted DMR were digested with the appropriate restriction endonucleases and were then separated using the MultiNA Microchip Electrophoresis System (Shimazdu, Japan). The methylation index was also calculated. All PCR primer sets used in this study have been listed in Supplementary Table SI (See Supporting Information online).

DNA Polymorphism Analyses

For quantitative polymorphism analyses, tetranucleotide repeat markers (*D11S1997* and *HUMTH01*) and a triplet repeat marker (*D11S2362*) from 11p15.4–p15.5 were amplified and separated by electrophoresis on an Applied Biosystems 3130 genetic analyzer (Applied Biosystems, NY); data were quantitatively analyzed with the GeneMapper software. The peak height ratios of paternal allele to maternal allele were calculated. A single nucleotide polymorphism (SNP) for the *Rsa*I recognition site in *H19* exon 5 (rs2839703) was also quantitatively analyzed using hot-stop PCR [Uejima et al., 2000]. Band intensity was measured using the FLA-7000 fluoro-image analyzer (Fujifilm).

Mutation Search of H19-DMR

To search for mutations in the binding sites of CTCF, OCT4, and SOX2, we sequenced a genomic region in and around H19-DMR, which included seven CTCF-binding sites, three OCT4 sites, and one SOX2 site.

TABLE I. Clinical Information of BWS Patients

Patient ID	Conception	Birth weight (gestational age)	Clinical features	Karyotype	Placental weight and pathology	Placental–fetal weight ratio
Patient 1 (BWS047)	Natural	4,506 g (36w2d)	macrosomia macroglossia abdominal wall defect hypoglycemia	46,XY	1,065 g no pathological findings	0.236
Patient 2 (bwsh21-015)	Natural	2,540 g (33w5d)	macrosomia macroglossia hypoglycemia renal malformation hepatosplenomegaly	46,XX	1,620 g placental chorangioma	0.638

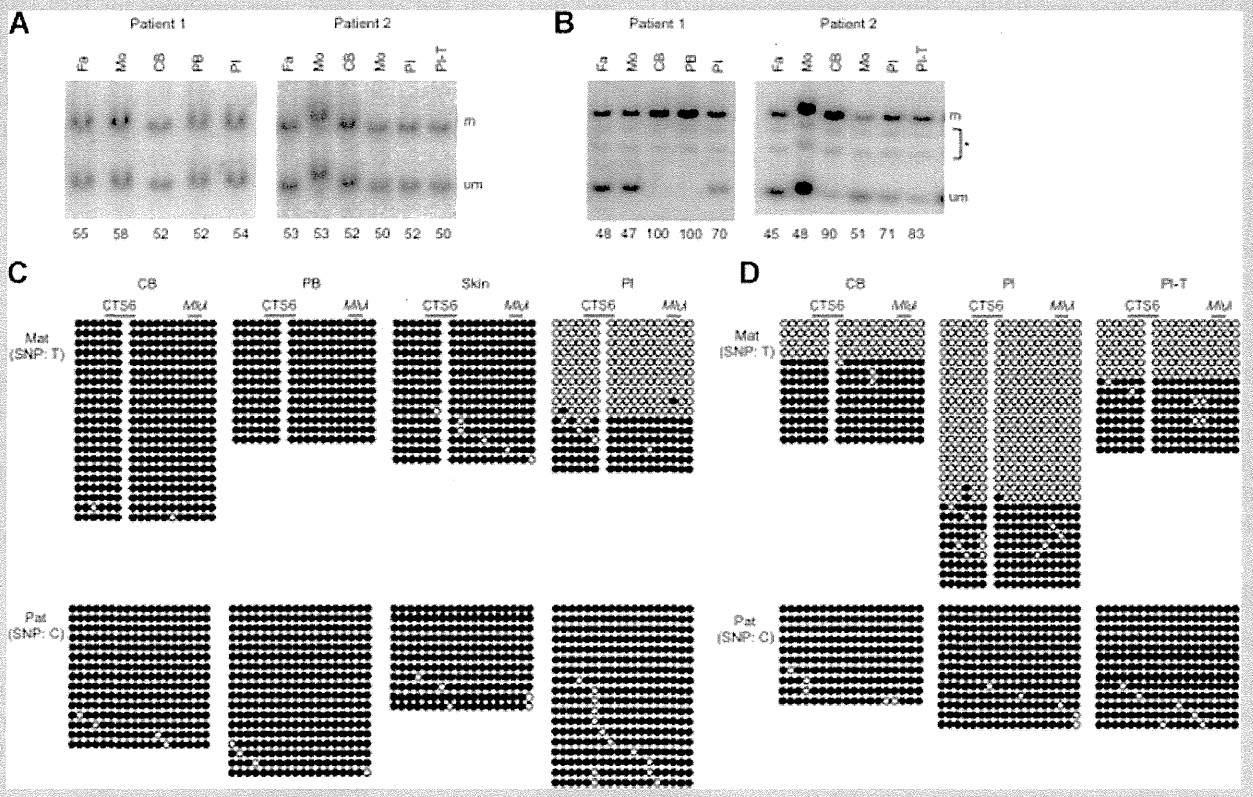

FIG. 1. Methylation analyses of KvDMR1 and H19-DMR. A: Methylation-sensitive Southern blots for KvDMR1. Genomic DNA was extracted from the cord blood, peripheral blood, skin, and placenta of Patient 1 and from the cord blood, placenta, and placental chorangioma of Patient 2. Methylation at KvDMR1 was normal in all samples analyzed. Methylation indices (MI, %) are shown under the figure. B: Methylation-sensitive Southern blots for H19-DMR. The MIs of blood samples were higher than the MIs of placental samples. MI was calculated using the equation [M/(M + U)] × 100, where M is the intensity of the methylated band and U is the intensity of the unmethylated band. C: Bisulfite sequencing of H19-DMR in Patient 1. The two parental alleles were distinguishable by differences in SNPs. Both parental alleles were completely methylated in the cord blood, peripheral blood, and skin samples, and the maternal allele, which is normally unmethylated, was partially methylated in the placenta. D: Bisulfite sequencing of H19-DMR in Patient 2. Methylation of the maternal allele was higher in the cord blood than in the placenta or placental chorangioma. These results were consistent with the results of the Southern blot analysis. We confirmed complete methylation of paternal H19-DMR alleles and complete demethylation of maternal H19-DMR alleles in four normal control placentas that were heterozygous for identifiable SNPs (data not shown). Fa, father; Mo, mother; CB, cord blood; PB, peripheral blood; PI, placenta; PI-T, placental chorangioma; m, methylated band; um, unmethylated band; *, nonspecific bands; Mat, maternal allele; Pat, paternal allele; CTS6, sixth CTCF binding site; *MluI*, a restriction site approximately 80 bp downstream of CTS6 assayed by methylation-sensitive Southern blot and COBRA.

RESULTS

We first examined the methylation status of the two ICRs, KvDMR1, and H19-DMR, at 11p15.5 using methylation-sensitive Southern blot analysis. Methylation at KvDMR1 was normal in all samples collected (Fig. 1A); however, methylation at H19-DMR was aberrant (Fig. 1B). In Patient 1, hypermethylation at H19-DMR was complete in cord blood and peripheral blood samples (MI = 100%), and hypermethylation in the placenta was partial (MI = 70%). In Patient 2, H19-DMR was partially hypermethylated in cord blood (MI = 90%) but less so in the placenta and placental chorangioma (MI = 71% and MI = 83%, respectively). For further investigation of differences in methylation between the patients' somatic tissues and placentas, the CTS6 site was subjected to bisulfite sequencing (Fig. 1C and D). We could distinguish the two parental alleles in each patient sample using informative SNPs (rs10732516 and rs2071094). The maternal allele, which is normally unmethylated, was completely methylated in the cord blood, peripheral blood, and skin from Patient 1. However, in placental samples from Patient 1, the maternal allele was only partially methylated: 36% of all CpGs analyzed were methylated. Similar results were observed in Patient 2: the maternal allele in the cord blood was 68% methylated; however, the maternal allele was only 31% and 55% methylated in the placenta and chorangioma samples, respectively. The paternal alleles, which are normally fully methylated, were fully methylated in all samples. These findings supported the results of the Southern blots. Furthermore, we could not find any microdeletions or mutations in or around H19-DMR,

including seven CTCF-binding sites, three OCT4 sites, and one SOX2 site, indicating that there was no genetic cause of the hypermethylation (Fig. 2A and data not shown).

Next, we analyzed polymorphic markers at 11p15.4–p15.5 to determine whether copy number abnormalities or paternal UPD might be involved in these BWS patients. Although smaller PCR products were more easily amplified, paternal–maternal allele ratios in blood samples were between 0.92 and 1.33, indicating that both parental alleles were equally represented in both patients (Fig. 2B). Therefore, we could rule out copy number abnormality and paternal UPD within the patients' blood. We also investigated maternal contamination in the placenta. *D11S1997* and *HUMTH01* for Patient 1 and the *Rsa*I polymorphism in *H19* (rs2839703) for Patient 2 were used for this investigation because the mothers were expected to be homozygous for such polymorphisms. Thus, we investigated contamination of our samples by assessing the homozygosity of the polymorphisms in the mothers. The paternal–maternal ratios in Patient 1 were 0.94 and 1.03, indicating an equal contribution of both parental alleles and suggesting no contamination (Fig. 2B). In Patient 2, the ratios were 0.77 and 0.78 in the placenta and chorangioma, respectively, suggesting a small amount of contamination (Fig. 2C). However, such contamination was too

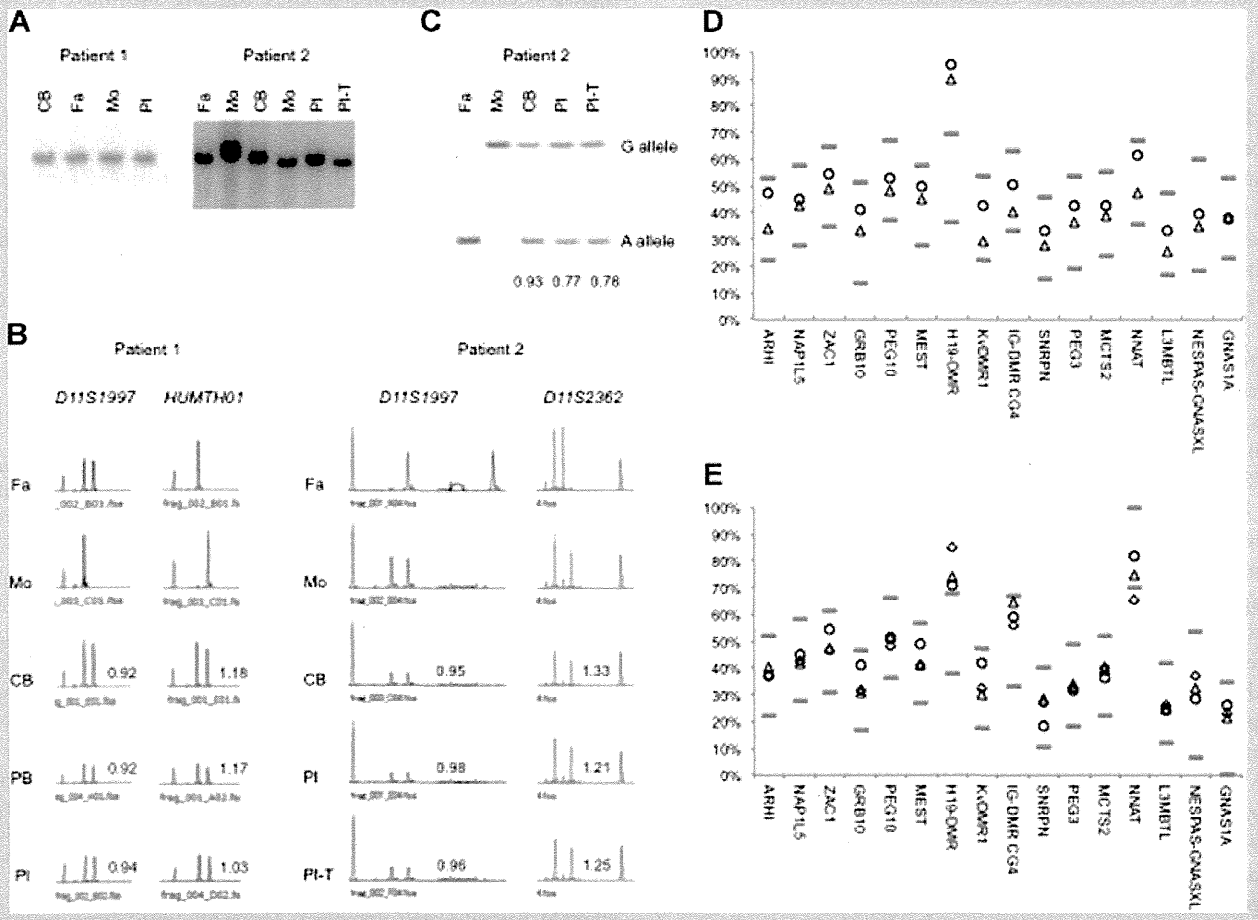

FIG. 2. Microdeletion analysis of H19-DMR, polymorphism analyses, and COBRA of primary imprinted DMRs in embryo-derived and placental samples. A: Southern blots identifying a microdeletion of H19-DMR. A genomic fragment (7.7 kb) generated by *Apa*I digestion, which included the entire H19-DMR, was evident in all samples, indicating that there was no microdeletion in this DMR. B: Microsatellite markers at 11p15.4–p15.5. The peak heights associated with each parental allele in all samples were quantitatively analyzed. The results indicated that both parental alleles were present and equally represented. C: Hot-stop PCR of an *Rsa*I polymorphic site in Patient 2. The ratios of paternal allele to maternal allele are shown under the figure. Although the ratios in the placenta and placental chorangioma are lower than in the cord blood, suggesting a small amount of maternal contamination, this was not enough to affect the results of the methylation analyses. COBRA of cord blood (D) and placentas (E), demonstrating that H19-DMR was hypermethylated. CTS6 is contained within H19-DMR. Methylation at other DMRs was normal in all samples, except for methylation at NNAT, which was aberrant in the placental chorangioma. Cord blood and placentas from 24 normal individuals were used as controls. The upper limit of normal methylation was defined as the higher of these two values: (1) the average of controls + 3 SD, or (2) the average + 15%. Similarly, the lower limit of normal methylation was definite as the lower of these two values: (1) the average of controls − 3 SD, or (2) the average − 15%. The upper and lower limits are indicated by gray bars. ○: Patient 1; △: Patient 2; ◇: placental chorangioma of Patient 2.

small to affect the results of the methylation analyses. In addition, sequence analysis did not show any mutations in *CDKN1C* (data not shown). These findings indicated that H19-DMR was aberrantly hypermethylated in both BWS patients and their associated placentas, but the aberrant methylation was consistently lower in the placenta, and that the H19-DMR GOM was strictly an isolated epimutation.

Finally, we analyzed the methylation status of 16 primary imprinted DMRs scattered throughout the genome-using COBRA (Fig. 2D and E). Only H19-DMR showed aberrant methylation among all primary DMRs in all samples, except for NNAT DMR, which was abnormal only in the placental chorangioma, indicating that the *IGF2/H19* imprinted domain was targeted for aberrant methylation in both somatic tissues and the placenta.

DISCUSSION

Methylation associated with parental imprints are erased in PGC and reestablished during gametogenesis in a sex-specific manner. The paternal pronucleus in the zygote undergoes active demethylation; extensive passive demethylation then ensues on maternal and paternal chromosomes during the pre-implantation period. After implantation, de novo methylation results in a rapid increase in DNA methylation in the inner cell mass (ICM), which gives rise to the entire embryo; in contrast, de novo methylation is either inhibited or not maintained in the trophoblast, which gives rise to the placenta [Li, 2002; Sasaki and Matsui, 2008]. The imprinted DMRs, however, escape these demethylation and de novo methylation events that occur in early embryogenesis. H19-DMR GOM in BWS patients is considered an error in imprint erasure in female PGCs [Horsthemke, 2010]. However, H19-DMR GOM, whether with or without microdeletions within H19-DMR, was partial, indicating a mosaic of normal cells and aberrantly methylated cells [Sparago et al., 2007; Cerrato et al., 2008]. These findings demonstrated that aberrant hypermethylation at H19-DMR was acquired after fertilization, although the precise timing was unknown.

Both participants in this study had isolated GOM at H19-DMR. The partial and variable hypermethylation among samples suggested epigenetic mosaicism. Furthermore, methylation levels in the placentas were lower than those in the blood and skin, suggesting that the aberrant methylation was acquired after implantation—when genome-wide de novo methylation normally occurs. Aberrant de novo methylation at H19-DMR is expected to be more widespread in the embryo than in the placenta, as this is normally the case for de novo methylation [Li, 2002; Sasaki and Matsui, 2008]; this disparity in efficiency could lead to the discordance between hypermethylation in trophoblast-derived placenta and that in embryo-derived blood and skin. This hypothesis is supported by a mouse experiment in which a mutant maternal allele harboring a deletion of four CTCF binding sites was hypomethylated in oocytes and blastocysts, yet was highly methylated after implantation [Engel et al., 2006]. To our knowledge, this is the first evidence demonstrating that aberrant hypermethylation of maternal H19-DMR is acquired after implantation in humans.

We found that of 16 primary imprinted DMRs analyzed, only H19-DMR showed aberrant methylation; even methylation at IG-DMR CG4, another paternally methylated, primary imprinted DMR, was normal in our patients. Although we only studied two patients, this finding indicated that the *IGF2/H19* imprinted domain in both the embryo and placenta was more susceptible than other imprinted domains to aberrant methylation acquired after implantation.

In conclusion, we found that methylation of H19-DMR was discordant in embryo-derived somatic tissue and placenta, strongly suggesting that the aberrant de novo methylation occurred after implantation. However, the precise mechanism of isolated H19-DMR GOM is still unknown. Since no mutations in *CTCF*, an important trans-acting imprinting factor, were found in these patients with isolated GOM at H19-DMR, the potential for mutations in the OCT and SOX transcription factors should be investigated because mutations of OCT-binding sites have previously been found in a few patients with H19-DMR GOM [Cerrato et al., 2008; Demars et al., 2010].

ACKNOWLEDGMENTS

This study was supported, in part, by a Grant-in-Aid for Scientific Research (C) (No. 20590330) from the Japan Society for the Promotion of Science, a Grant for Research on Intractable Diseases from the Ministry of Health, Labor, and Welfare, and a Grant for Child Health and Development from the National Center for Child Health and Development.

REFERENCES

Aoki A, Shiozaki A, Sameshima A, Higashimoto K, Soejima H, Saito S. 2011. Beckwith–Wiedemann syndrome with placental chorangioma due to H19-differentially methylated region hypermethylation: A case report. J Obstet Gynaecol Res 37:1872–1876.

Bell AC, Felsenfeld G. 2000. Methylation of a CTCF-dependent boundary controls imprinted expression of the Igf2 gene. Nature 405:482–485.

Cerrato F, Sparago A, Verde G, De Crescenzo A, Citro V, Cubellis MV, Rinaldi MM, Boccuto L, Neri G, Magnani C, D'Angelo P, Collini P, Perotti D, Sebastio G, Maher ER, Riccio A. 2008. Different mechanisms cause imprinting defects at the IGF2/H19 locus in Beckwith–Wiedemann syndrome and Wilms' tumour. Hum Mol Genet 17:1427–1435.

Demars J, Shmela ME, Rossignol S, Okabe J, Netchine I, Azzi S, Cabrol S, Le Caignec C, David A, Le Bouc Y, El-Osta A, Gicquel C. 2010. Analysis of the IGF2/H19 imprinting control region uncovers new genetic defects, including mutations of OCT-binding sequences, in patients with 11p15 fetal growth disorders. Hum Mol Genet 19:803–814.

Elliott M, Bayly R, Cole T, Temple IK, Maher ER. 1994. Clinical features and natural history of Beckwith–Wiedemann syndrome: Presentation of 74 new cases. Clin Genet 46:168–174.

Engel N, Thorvaldsen JL, Bartolomei MS. 2006. CTCF binding sites promote transcription initiation and prevent DNA methylation on the maternal allele at the imprinted H19/Igf2 locus. Hum Mol Genet 15:2945–2954.

Hark AT, Schoenherr CJ, Katz DJ, Ingram RS, Levorse JM, Tilghman SM. 2000. CTCF mediates methylation-sensitive enhancer-blocking activity at the H19/Igf2 locus. Nature 405:486–489.

Horsthemke B. 2010. Mechanisms of imprint dysregulation. Am J Med Genet C Semin Med Genet 154C:321–328.

Li E. 2002. Chromatin modification and epigenetic reprogramming in mammalian development. Nat Rev Genet 3:662–673.

Sasaki H, Matsui Y. 2008. Epigenetic events in mammalian germ-cell development: Reprogramming and beyond. Nat Rev Genet 9:129–140.

Sasaki K, Soejima H, Higashimoto K, Yatsuki H, Ohashi H, Yakabe S, Joh K, Niikawa N, Mukai T. 2007. Japanese and North American/European patients with Beckwith–Wiedemann syndrome have different frequencies of some epigenetic and genetic alterations. Eur J Hum Genet 15: 1205–1210.

Soejima H, Nakagawachi T, Zhao W, Higashimoto K, Urano T, Matsukura S, Kitajima Y, Takeuchi M, Nakayama M, Oshimura M, Miyazaki K, Joh K, Mukai T. 2004. Silencing of imprinted CDKN1C gene expression is associated with loss of CpG and histone H3 lysine 9 methylation at DMR-LIT1 in esophageal cancer. Oncogene 23:4380–4388.

Sparago A, Cerrato F, Vernucci M, Ferrero GB, Silengo MC, Riccio A. 2004. Microdeletions in the human H19 DMR result in loss of IGF2 imprinting and Beckwith–Wiedemann syndrome. Nat Genet 36:958–960.

Sparago A, Russo S, Cerrato F, Ferraiuolo S, Castorina P, Selicorni A, Schwienbacher C, Negrini M, Ferrero GB, Silengo MC, Anichini C, Larizza L, Riccio A. 2007. Mechanisms causing imprinting defects in familial Beckwith–Wiedemann syndrome with Wilms' tumour. Hum Mol Genet 16:254–264.

Uejima H, Lee MP, Cui H, Feinberg AP. 2000. Hot-stop PCR: A simple and general assay for linear quantitation of allele ratios. Nat Genet 25: 375–376.

Weksberg R, Nishikawa J, Caluseriu O, Fei YL, Shuman C, Wei C, Steele L, Cameron J, Smith A, Ambus I, Li M, Ray PN, Sadowski P, Squire J. 2001. Tumor development in the Beckwith–Wiedemann syndrome is associated with a variety of constitutional molecular 11p15 alterations including imprinting defects of KCNQ1OT1. Hum Mol Genet 10:2989–3000.

Weksberg R, Shuman C, Beckwith JB. 2010. Beckwith–Wiedemann syndrome. Eur J Hum Genet 18:8–14.

Original Paper

Cells Tissues Organs

Cells Tissues Organs
DOI: 10.1159/000342806

Accepted after revision: August 17, 2012
Published online: November 3, 2012

Human Chorionic Gonadotropin Induces Human Macrophages to Form Intracytoplasmic Vacuoles Mimicking Hofbauer Cells in Human Chorionic Villi

Munekage Yamaguchi[a] Takashi Ohba[a] Hironori Tashiro[a] Gen Yamada[b] Hidetaka Katabuchi[a]

[a]Department of Obstetrics and Gynecology, Faculty of Life Sciences, and [b]Department of Organ Formation, Institute of Molecular Embryology and Genetics, Kumamoto University, Kumamoto, Japan

Key Words

Hofbauer cells · Macrophages · Human chorionic gonadotropin · Luteinizing hormone/chorionic gonadotropin receptor · Chorionic villi · Placenta

Abstract

The most characteristic morphological feature of macrophages in the stroma of placental villi, known as Hofbauer cells, is their highly vacuolated appearance. They also show positive immunostaining for human chorionic gonadotropin (hCG) and express messenger ribonucleic acid of the luteinizing hormone/chorionic gonadotropin receptor with a deletion of exon 9 (LH/CG-R Δ9). Maternal hCG enters fetal plasma through the mesenchyme of the placental villi and promotes male sexual differentiation in early pregnancy; therefore, excess hCG may induce aberrant genital differentiation and hCG must be adjusted at the fetomaternal interface. We hypothesized that hCG is regulated by Hofbauer cells and that their peculiar vacuoles are involved in a cell-specific function. To assess the morphological modification and expression of LH/CG-R Δ9 in human macrophages after hCG exposure, the present study examined phorbol 12-myristate 13-acetate (PMA)-treated THP-1 cells, a human monocyte-macrophage cell line. hCG induced transient vacuole formation in PMA-treated THP-1 cells, morphologically mimicking Hofbauer cells. Immunocytochemistry showed that PMA-treated THP-1 cells incorporated hCG but not luteinizing hormone or follicle-stimulating hormone. Western blotting analyses demonstrated that PMA-treated THP-1 cells expressed an immunoreactive 60-kDa protein, designated as endogenous LH/CG-R Δ9. hCG induced a transient reduction in the LH/CG-R Δ9, which was synchronous with the appearance of cytoplasmic vacuoles. In conclusion, human macrophages regulating hCG via cytoplasmic LH/CG-R Δ9 mimic the morphological characteristics of Hofbauer cells. Their vacuoles may be associated with their cell-specific function to protect the fetus from exposure to excess maternal hCG during pregnancy.

Introduction

Resident tissue macrophages differentiated from blood monocytes adapt to their local environment to perform specific functions in organs and tissues [Hume et al., 2002]. Macrophages in the stroma of placental villi, known as Hofbauer cells, are characterized by a peculiar vacuolated form [Castellucci and Kaufmann, 2006],

KARGER

Fax +41 61 306 12 34
E-Mail karger@karger.ch
www.karger.com

1422–6405/12/0000–0000$38.00/0

Accessible online at:
www.karger.com/cto

Dr. Munekage Yamaguchi
Department of Obstetrics and Gynecology
Faculty of Life Sciences, Kumamoto University
1-1-1 Honjyo, Chuou-Ku, Kumamoto-City, Kumamoto 860-8556 (Japan)
E-Mail munekage@hotmail.co.jp

Abbreviations used in this paper

bp	base pairs
CD	cluster of differentiation
FSH	follicle-stimulating hormone
hCG	human chorionic gonadotropin
GAPDH	glyceraldehyde 3-phosphate dehydrogenase
HE	hematoxylin and eosin
HRP	horseradish peroxidase
LDL	low-density lipoprotein
LH	luteinizing hormone
LH/CG-R	luteinizing hormone/chorionic gonadotropin receptor
LH/CG-R Δ9	luteinizing hormone/chorionic gonadotropin receptor with a deletion of exon 9
mRNA	messenger ribonucleic acid
PMA	phorbol 12-myristate 13-acetate
RT-PCR	reverse transcription-polymerase chain reaction
TBST	Tris-buffered saline containing 0.05% Tween 20

which is not observed in human macrophages distributed in other organs. Despite the identification of Hofbauer cells more than 100 years ago, their functions and the physiological roles of the vacuoles are still not well understood.

Hofbauer cells are found in the stroma adjacent to human chorionic gonadotropin (hCG)-producing trophoblasts and fetal capillaries, and their cytoplasmic vacuoles may be associated with phagocytic activity [Ingman et al., 2010]. Moreover, they may maintain host defense to prevent pathogens, toxins and immunological complexes from reaching the fetus [Frauli and Ludwig, 1987; Ingman et al., 2010]. Hofbauer cells show positive immunohistochemical staining with hCG [Katabuchi et al., 1989, 1994], thus suggesting that hCG is phagocytosed from the surrounding environment because macrophages are thought to be unable to synthesize hCG [Castellucci and Kaufmann, 2006]. Fetal plasma concentrations of total hCG are only 3% of the maternal plasma levels, ranging from 30 to 2,800 mIU/ml between 8 and 20 weeks of gestation [Clements et al., 1976]. Circulating hCG in fetal blood is necessary for the differentiation of the fetal genitalia; therefore, excess hCG may induce aberrant genital differentiation of the fetus [Huhtaniemi et al., 1977; Takasugi et al., 1985; Matzuk et al., 2003]. We thus hypothesized that macrophages in placental villi regulate hCG to prevent the fetus from excess maternal hCG and the peculiar cytoplasmic vacuoles are related to the cell-specific function of Hofbauer cells.

Khan et al. [2000] first demonstrated that human macrophages could take up and degrade hCG by culturing human peritoneal macrophages. Sonoda et al. [2005] confirmed the degradation of hCG by phorbol 12-myristate 13-acetate (PMA)-treated THP-1 cells, which were established from human acute monocytic leukemia cells as a human monocyte-macrophage lineage cell line. They subsequently revealed that both PMA-treated THP-1 cells and Hofbauer cells expressed only a messenger ribonucleic acid (mRNA) encoding the variant type of luteinizing hormone/chorionic gonadotropin receptor (LH/CG-R) with a deletion of exon 9 (LH/CG-R Δ9) and that the ability of PMA-treated THP-1 cells to degrade hCG was impaired by transfection of full-length LH/CG-R mRNA [Sonoda et al., 2005]. Although these results suggested that endogenous LH/CG-R Δ9 was involved in the regulation of hCG in human macrophages, they could not confirm whether LH/CG-R Δ9 protein was produced from the endogenous gene and regulated hCG in human macrophages. The current study assessed the morphological changes and expression of LH/CG-R Δ9 in PMA-treated THP-1 cells after hCG exposure.

Materials and Methods

THP-1 Cell Culture and Gonadotropin Treatment

THP-1 cells were obtained from the American Type Culture Collection. They adhere to plastic dishes in culture medium and change into amoeboid cells with the characteristics of macrophages when treated with PMA (Sigma-Aldrich, Japan). THP-1 cells were first maintained in suspension cultures in Roswell Park Memorial Institute (RPMI)-1640 medium (Gibco, Japan) containing 10% heat-inactivated fetal bovine serum, 50 U/ml penicillin (Gibco), and 50 mg/ml streptomycin sulfate (Gibco) at 37°C in 5% CO_2 and 95% air. The cells were incubated in 60-mm dishes (BD Falcon, Japan) at a concentration of 1×10^6 cells/ml for 24 h in medium supplemented with 1.6×10^{-7} M PMA to induce their differentiation into macrophages. The cells were extensively washed with phosphate-buffered saline (pH 7.2), then cultured in RPMI-1640 medium containing 10% fetal bovine serum again and subsequently exposed to 1,000 mUI/ml of hCG (Mochida, Japan), luteinizing hormone (LH; Sigma-Aldrich, Japan) or follicle-stimulating hormone (FSH; Sigma-Aldrich). The concentration of hCG was determined according to the reported fetal plasma concentrations [Clements et al., 1976]. LH and FSH were used at the same concentration to compare the differences with hCG. Liquid culture media containing gonadotropin were removed by suction at the following defined periods; 1, 15, 30 min, 1, 2 or 3 h. The adherent cells in all dishes were extensively washed with phosphate-buffered saline, and then were used in the subsequent experiments.

Paraffin Embedding of Cell Block Specimens

The adherent cells without or with gonadotropin treatment were detached from the dishes using a cell scraper (BD Falcon) with 500 μl of trypsin-ethyleneaminetetraacetic acid solution (Gibco), and fixed in 10% neutral buffered formalin. The cells were suspended in 1% sodium arginate and solidified by the addition of 1 M calcium chloride. Finally, gelatinous specimens containing PMA-treated THP-1 cells without or with gonadotropin treatment were embedded in paraffin and cut into 4-μm sections.

Tissue Collection

Tissues of the chorionic villi were obtained from a normal pregnant woman undergoing an artificial abortion in early pregnancy. Informed consent was obtained from the patient. Ethical approval was also obtained and this study was performed according to the guidelines of the Ethics Committee in Faculty of Life Science, Kumamoto University. The tissue sample was fixed in 10% neutral buffered formalin for 24 h, embedded in paraffin and cut into 4-μm sections.

Hematoxylin and Eosin Staining, Immunocytochemistry and Immunofluorescence Analyses

A paraffin-embedded section of chorionic villi and 6 paraffin-embedded sections of cell blocks were stained with hematoxylin and eosin (HE). A paraffin-embedded section of chorionic villi was immunohistochemically stained with 3.7 μg/ml of mouse anti-cluster of differentiation (CD) 68 monoclonal antibody (Dako, Japan). Nine paraffin-embedded sections of cell blocks were immunocytochemically stained with 3.7 μg/ml of mouse anti-CD68 monoclonal antibody (Dako), 14.2 μg/ml of rabbit anti-hCG-β polyclonal antibody (Dako), 0.1 μg/ml of mouse anti-LH-β monoclonal antibody (Thermo Scientific, Japan), 0.4 μg/ml of mouse anti-FSH-β monoclonal antibody (Thermo Scientific, Japan) or 1.0 μg/ml of rabbit anti-human LH/CG-R polyclonal antibody which was raised against amino acids 28–77 (exon 1) mapping to an extracellular domain of LH/CG-R of human origin (Santa Cruz Biotechnology, Calif., USA). For immunocytochemistry, horseradish peroxidase-labeled goat anti-rabbit or mouse immunoglobulins were used for 60 min as secondary antibodies. The peroxidase activity was visualized with Immpact DAB Diluent (Vector Laboratories, USA). Nuclear staining was performed with 1% methyl green in water. For immunofluorescence analyses, anti-rabbit or mouse Alexa Fluor 488 were used for 90 min as secondary antibodies. 4′,6-Diamidino-2-phenylindole (Roche, Japan) was used for detection of nuclei. Sections were viewed with a Biorevo BZ-9000 fluorescence microscope (Keyence, Japan). Negative controls were prepared by replacing the primary antibody with nonimmune antiserum from rabbits or mice.

Isolation of mRNA and Reverse Transcription-Polymerase Chain Reaction

Total RNA was extracted from cells and the chorionic villi obtained from the placenta by using RNeasy Mini Kit (Qiagen, Japan), according to the manufacturer's protocols. Complementary deoxyribonucleic acid (cDNA) was synthesized using the SuperScript III Transcriptor First Strand cDNA Synthesis System for RT-PCR (Invitrogen, Japan), according to the manufacturer's instructions.

PCR was performed using KOD-Plus-Neo kit (Toyobo Co., Japan) on a Thermal Cycler PTC-200 (Bio-Rad, Japan). Two different primers for PCR were designed specific for hCG-β gene 7 and 8 products, respectively (all forward then reverse primer): hCG-β1 5′-TCACTTCACCGTGGTCTCCG-3′ and 5′-TGCAGCACGCGGGTCATGGT-3′ [423 base pairs (bp)] with 10 s at 98°C, 30 s at 60°C and 30 s at 68°C for 35 cycles; hCG-β2 5′-TGGCTGTGGAGAAGGAGGGCTGC-3′ and 5′-GGAAGCGGGGGTCATCACAGGTC-3′ (300 bp) with 10 s at 98°C, 30 s at 64°C and 30 s at 72°C for 35 cycles. Glyceraldehyde 3-phosphate dehydrogenase (GAPDH) was used for control with same condition as hCG-β1.

Western Blot Analysis

The adherent cells without or with gonadotropin treatment were solubilized in 500 μl of Laemmli sample buffer (Bio-Rad, Japan) containing Complete Mini-Protease Inhibitors (Roche, Japan) and β-mercaptoethanol (1:20). The protein concentrations were determined by a Bradford assay [Bradford, 1976]. A total of 20 μl of protein extracts from these cells were loaded onto a reducing 10% sodiumdodecyl sulfate-tris(hydroxymethyl)aminomethane (Tris) polyacrylamide gel (Bio-Rad), and transferred to nitrocellulose membranes (Bio-Rad). The membranes were briefly washed in Tris-buffered saline containing 0.05% Tween 20 (TBST) and nonspecific binding sites were blocked by immersing the membranes in skim milk (Yukijirushi, Japan) for 1 h at room temperature on an orbital shaker. The membranes were shortly rinsed in two changes of TBST, and washed once for 15 min and twice for 5 min in fresh changes of TBST. The membranes were subjected to 1.0 μg/ml of rabbit anti-human LH/CG-R polyclonal antibody in blocking reagent for 1 h at room temperature. The membranes were washed and incubated with the peroxidase-labeled goat anti-rabbit IgG for 1 h at room temperature. The membranes were washed 3 × 10 min in fresh changes of TBST. Bound antibodies were detected by a chemiluminescent detection system (Amersham, Japan) as recommended by the manufacturer's protocol. Amersham hyper film ECL (GE Healthcare, Japan) was used to capture the chemiluminescence (exposure for 1, 5 min, and up to 15 min).

Results

hCG-Induced Morphological Change in PMA-Treated THP-1 Cells

There were CD68-positive coarsely vacuolated cells in the stroma of the human chorionic villi in early gestation (fig. 1a, b), and it is generally agreed that these cells are macrophages, known as Hofbauer cells. We confirmed that CD68, a human macrophage marker, was also expressed in PMA-treated THP-1 cells (fig. 1c). In the cell blocks of PMA-treated THP-1 cells, small cells with scanty cytoplasm were observed without hCG and 15 min after the addition of hCG (fig. 2a, b). When PMA-treated THP-1 cells were exposed to hCG for 30 min, multiple cytoplasmic vacuoles of various sizes appeared in the cytoplasm (fig. 2c). These cells mimicked the structure of Hofbauer cells in early pregnancy. The vacuoles were decreased in number and partly became larger in size at

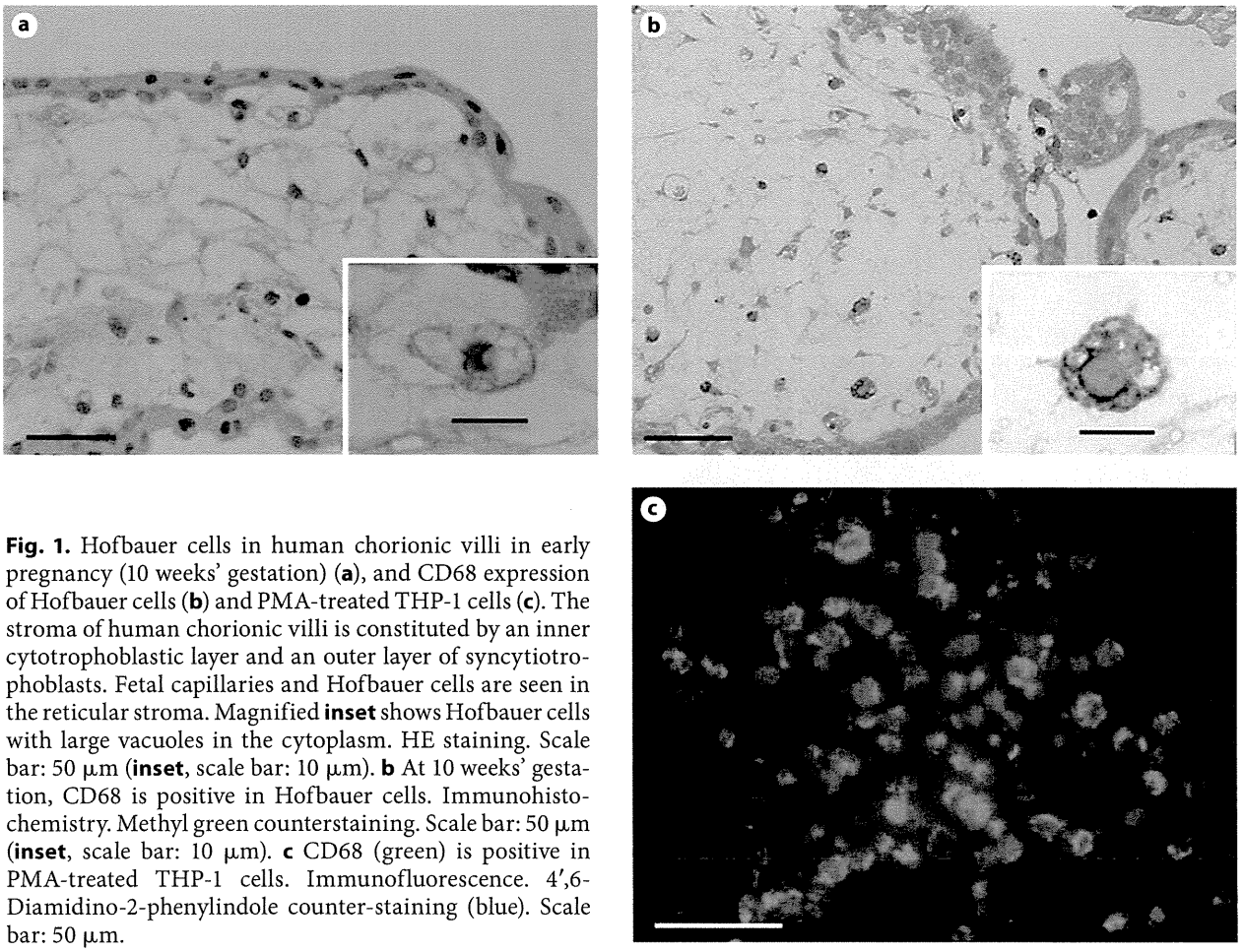

Fig. 1. Hofbauer cells in human chorionic villi in early pregnancy (10 weeks' gestation) (**a**), and CD68 expression of Hofbauer cells (**b**) and PMA-treated THP-1 cells (**c**). The stroma of human chorionic villi is constituted by an inner cytotrophoblastic layer and an outer layer of syncytiotrophoblasts. Fetal capillaries and Hofbauer cells are seen in the reticular stroma. Magnified **inset** shows Hofbauer cells with large vacuoles in the cytoplasm. HE staining. Scale bar: 50 μm (**inset**, scale bar: 10 μm). **b** At 10 weeks' gestation, CD68 is positive in Hofbauer cells. Immunohistochemistry. Methyl green counterstaining. Scale bar: 50 μm (**inset**, scale bar: 10 μm). **c** CD68 (green) is positive in PMA-treated THP-1 cells. Immunofluorescence. 4′,6-Diamidino-2-phenylindole counter-staining (blue). Scale bar: 50 μm.

1 and 2 h after hCG exposure (fig. 2d, e), and few vacuoles were observed at 3 h after hCG exposure (fig. 2f).

Selective Uptake of hCG by PMA-Treated THP-1 Cells

Immunocytochemistry showed that PMA-treated THP-1 cells before gonadotropin treatment were all negative against hCG, LH or FSH antibody (fig. 3a–c). On exposition to hCG for 1 min, hCG was positive in the cytoplasm of PMA-treated THP-1 cells (fig. 3d). In contrast to hCG, PMA-treated THP-1 cells showed negative staining with LH or FSH following exposure to LH or FSH in the same period (fig. 3e, f). Using specific oligonucleotide primer pairs in RT-PCR, we found that the expected hCG cDNA amplification products of 423 and 300 bp were not detected in both PMA-treated THP-1 cells without hCG and PMA-treated THP-1 cells 1 min after hCG exposure (fig. 3g). These results suggest that human macrophages are not involved in the production of hCG but in rapid and selective incorporation of hCG.

Endogenous LH/CG-R Δ9 Expression and Transient Reduced Expression by hCG in PMA-Treated THP-1 Cells

Immunocytochemistry demonstrated that LH/CG-R was strongly positive in the cytoplasm of PMA-treated THP-1 cells (fig. 4a). When the cells were exposed to hCG for 30 min, the cytoplasmic staining of LH/CG-R was weakened and cytoplasmic vacuoles appeared (fig. 4b).

A Western blotting analysis was conducted to determine the molecular size of the endogenous LH/CG-R. PMA-treated THP-1 cells expressed only a 60-kDa protein, designated as LH/CG-R Δ9 (fig. 5a). Next, the time course of LH/CG-R Δ9 expression was assessed after the administration of hCG. The expression of LH/CG-R Δ9 was transiently decreased from 30 min through 2 h after hCG exposure (fig. 5b). The reduction of LH/CG-R Δ9 was not induced by either LH or FSH exposure (fig. 6).

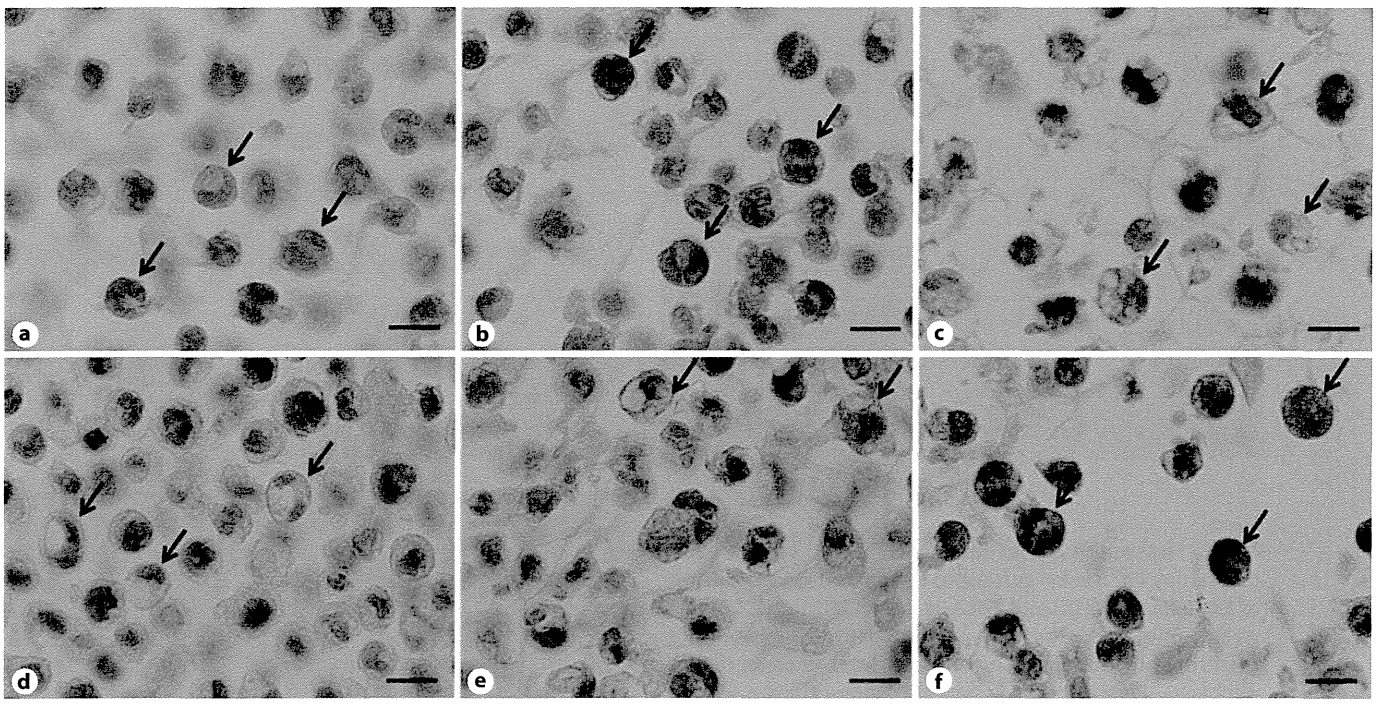

Fig. 2. Morphological changes in PMA-treated THP-1 cells after hCG exposure. PMA-treated THP-1 cells were exposed to 1,000 mIU/ml of hCG without hCG treatment (**a**), 15 min after hCG exposure (**b**), after 30 min (**c**), after 1 h (**d**), after 2 h (**e**), after 3 h (**f**). Few cytoplasmic vacuoles are seen in **a**, **b** and **f**. Multiple cytoplasmic vacuoles of various sizes are observed in **c**, and large vacuoles are partly seen in **d** and **e**. HE staining. Arrows indicate characteristic morphological feature in each panel. **a–f** Scale bar: 10 μm.

Discussion

Hofbauer cells are capable of both nonimmune and immune phagocytosis [Fox and Sebire, 2007a]. The placenta lacks a lymphatic system to return proteins from the interstitial space to the blood vascular system; therefore, intracytoplasmic vacuoles in Hofbauer cells have been considered to be associated with phagocytic activity to reduce serum proteins contained in the villous stroma and regulate the water in early placenta [Castellucci and Kaufmann, 2006]. They can also trap maternal immunoglobulins crossing over into the placental tissues and suppress the immune response to fetal transplantation antigens [Frauli and Ludwig, 1987; Fox and Sebire, 2007a]. Hence, it has been postulated that Hofbauer cells act as a secondary line of defense to prevent pathogens and toxins from reaching the fetus [Ingman et al., 2010]. Since excess hCG also has an adverse effect on the fetus, we hypothesized that Hofbauer cells phagocytose and regulate hCG and also that their peculiar cytoplasmic vacuoles are related to their cell-specific function. The present study first demonstrated that hCG elicited transient morphological changes, mimicking Hofbauer cells in PMA-treated THP-1 cells, suggesting that characteristic vacuoles in Hofbauer cells are associated with hCG-phagocytic activity.

The major role of hCG in early pregnancy is to maintain the corpus luteum for persistent progesterone production [Shi et al., 1993; Cunningham et al., 2005]. hCG is produced and secreted from placental syncytiotrophoblasts into the maternal circulation and is detectable in maternal plasma 7–10 days after implantation of the fertilized ovum. The maternal serum hCG levels rise very rapidly, to reach a transient peak at about 8–10 weeks of gestation. The level in this period is 1,000 times greater than the level 6 weeks earlier [Fox and Sebire, 2007b]. The levels of hCG begin to decline, and a nadir is reached by about 20 weeks of gestation. The plasma levels are maintained at this lower level for the remainder of pregnancy [Cunningham et al., 2005]. Circulating maternal hCG at the peak level enters in the fetal plasma and stimulates fetal testicular testosterone production. hCG acts

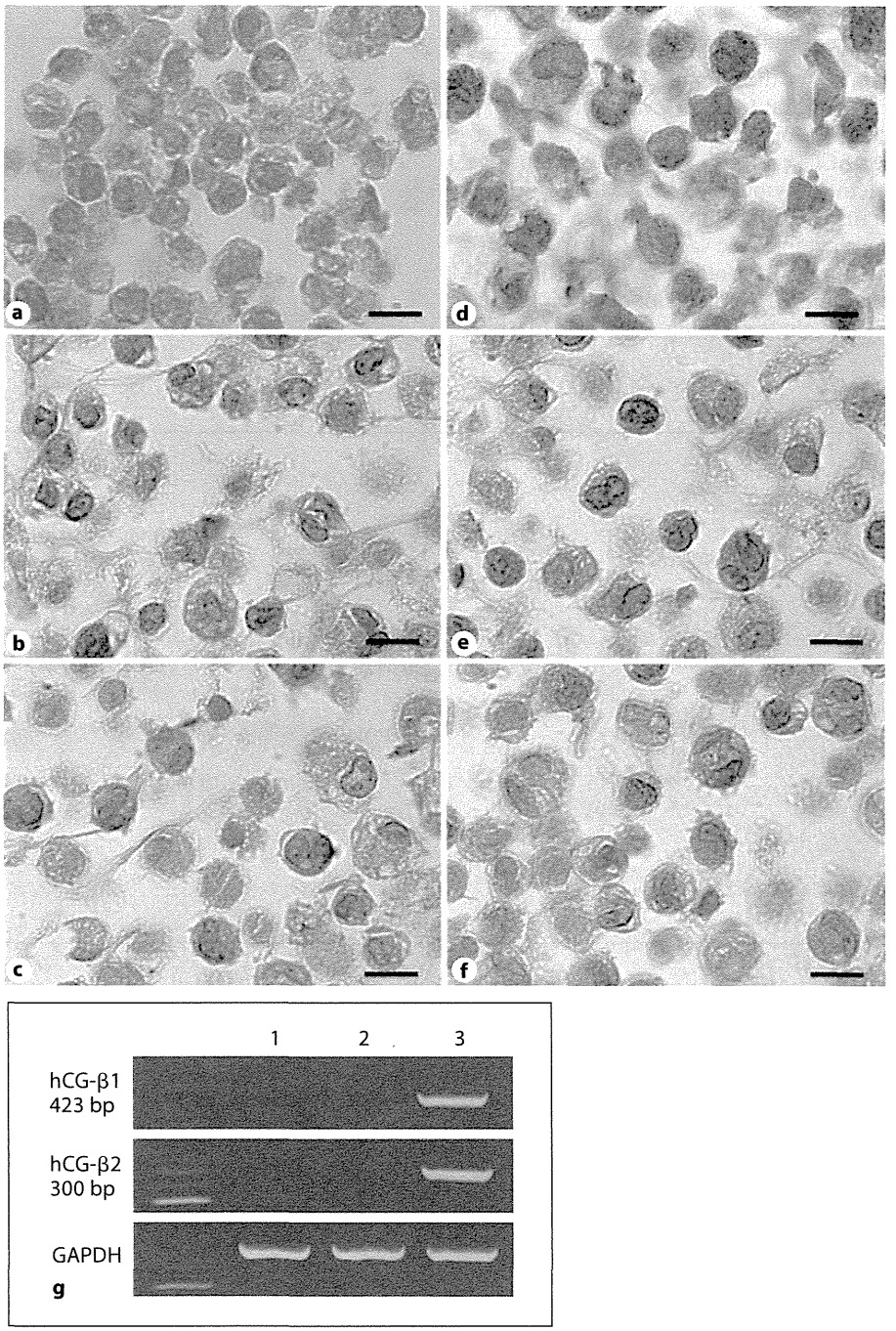

Fig. 3. Localization of gonadotropin and expression of hCG-β mRNA in PMA-treated THP-1 cells after gonadotropin exposure. **a–c** PMA-treated THP-1 cells without gonadotropin treatment. **d–f** PMA-treated THP-1 cells exposed to hCG (**d**), LH (**e**) or FSH (**f**) for 1 min. **g** Expression of hCG-β mRNA in PMA-treated THP-1 cells without hCG treatment (lane 1), PMA-treated THP-1 cells exposed to hCG for 1 min (lane 2) and the chorionic villi (lane 3) analyzed by RT-PCR. The cells were immunostained with anti-hCG-β antibody (**a**, **d**), anti-LH-β antibody (**b**, **e**) or anti-FSH-β antibody (**c**, **f**). **d** shows positive staining in the cytoplasm and the other panels all show negative staining. Neither hCG-β1 nor hCG-β2 mRNA is expressed in lanes 1 and 2. cDNA of the chorionic villi was amplified with primer for 423 and 300 bp showing the predicted hCG-β DNA products as positive control (lane 3). GAPDH was used as a control. Methyl green counterstaining. Scale bar: 10 μm.

as an LH surrogate and stimulates replication of testicular Leydig cells and testosterone synthesis to promote male sexual differentiation at a critical time in sexual differentiation of the male fetus [Huhtaniemi et al., 1977; Cunningham et al., 2005]. High-dose hCG exposure to mice offspring induce abnormal male and female gonadal development [Takasugi et al., 1985; Matzuk et al., 2003]; therefore, exposure to excess hCG has the possibility to cause ambiguous genital differentiations of human fetuses. In addition, the cytoplasm of Hofbauer cells is coarsely vacuolated during early pregnancy; however, as gestation progresses, the vacuoles decrease in number

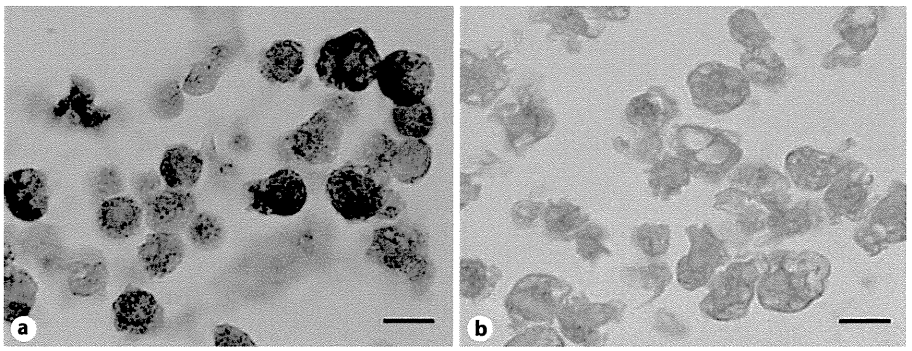

Fig. 4. Localization of LH/CG-R in PMA-treated THP-1 cells. **a** PMA-treated THP-1 cells without hCG treatment. **b** 30 min after hCG exposure, LH/CG-R is positive in their cytoplasm. LH/CG-R is weakly stained when compared with **a** and multiple cytoplasmic vacuoles of various sizes are observed. Both were immunostained with anti-LH/CG-R antibody. **a**, **b** Methyl green counterstaining. Scale bar: 10 μm.

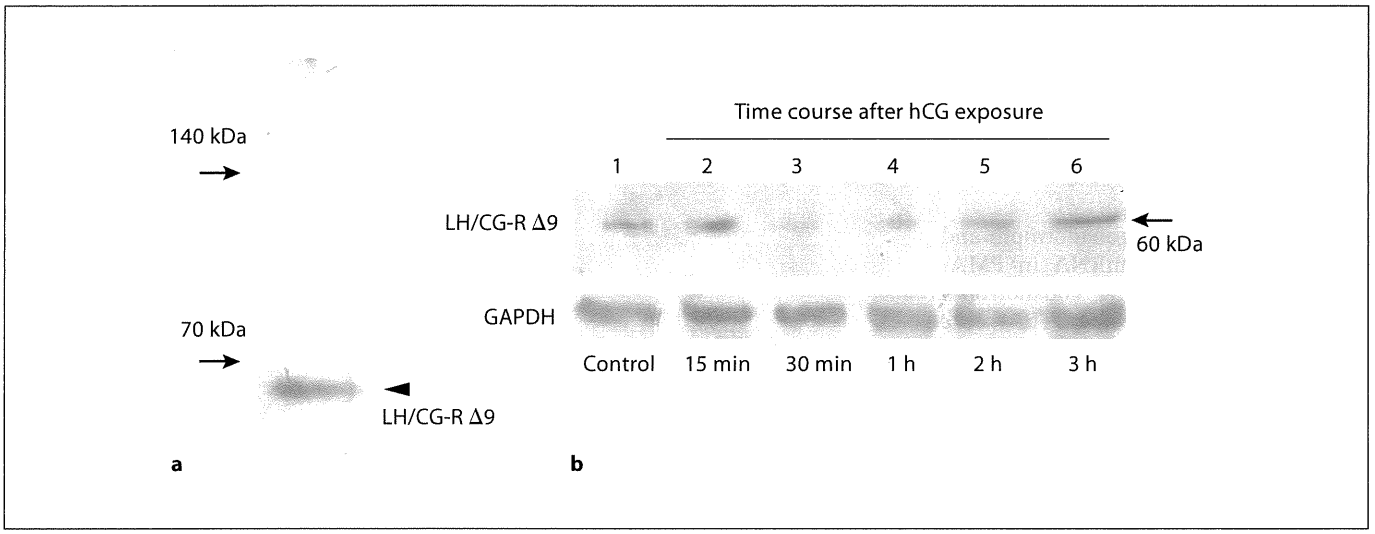

Fig. 5. Molecular weight and quantitative variation in LH/CG-R expression in PMA-treated THP-1 cells after hCG exposure. **a** LH/CG-R expression in PMA-treated THP-1 cells without hCG treatment. The arrowhead shows a protein band of 60 kDa. **b** Time course analysis of LH/CG-R expression in PMA-treated THP-1 cells after hCG exposure. Lane 1: control, lane 2: 15 min, lane 3: 30 min, lane 4: 1 h, lane 5: 2 h and lane 6: 3 h. The immunoreactive protein bands of lanes 1, 2, and 6 are visible; in contrast, those of lane 3, 4, and 5 are practically invisible. GAPDH was used as a control for protein loading.

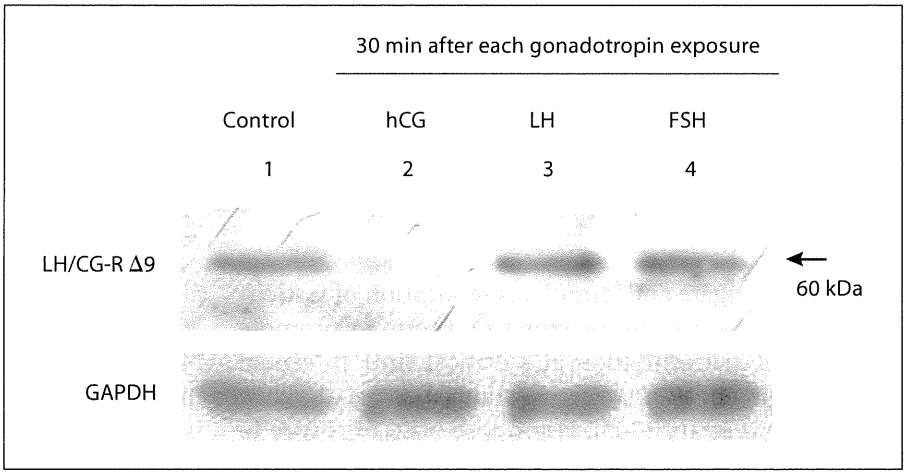

Fig. 6. Expression of LH/CG-R in PMA-treated THP-1 cells after exposure to gonadotropin. LH/CG-R expression in control (lane 1) and PMA-treated THP-1 cells 30 min after exposure to hCG (lane 2), LH (lane 3), or FSH (lane 4). The expression of LH/CG-R is decreased in only lane 2 compared with the control band. GAPDH was used as a control for protein loading.

and size [Castellucci and Kaufmann, 2006]. These findings indicate that the increased maternal hCG level is correlated with the increased number and size of vacuoles in Hofbauer cells. The correlation suggests that macrophages regulate peak levels of hCG during the first trimester and subsequently form characteristic cytoplasmic vacuoles.

In the present study, PMA-treated THP-1 cells quickly incorporated hCG, but not LH or FSH. This result suggests that human macrophages can distinguish hCG from LH or FSH on the cell surface. hCG, LH and FSH are dimers composed of two glycosylated polypeptide subunits, α and β. All of these human gonadotropic hormones share a common α-chain; therefore, the β-subunit determines the specific biologic activity of a glycopeptide hormone. hCG has the largest β-subunit, containing a larger carbohydrate moiety and 145 amino acid residues, including a unique carboxyl-terminal tail piece of 29 amino acid. Besides, hCG-β contains four additional sites for glycosylation in comparison with LH and FSH. This glycosylation makes hCG-β more negatively charged [Marc and Leon, 2011]. In early atherosclerotic lesions, macrophages do not take up native low-density lipoprotein but negatively charged oxidized low-density lipoprotein recognized by their scavenger receptors, subsequently forming foam cells [Steinberg and Witztum, 2010]. Intact hCG is more negatively charged in the early stage than in the late stage of gestation [Medeiros and Norman, 2009]. Human macrophages may recognize and incorporate more negatively charged hCG via transmembrane receptors, e.g. scavenger receptors.

The β-subunits of both hCG and LH have a high affinity for LH/CG-R, which plays a pivotal role in reproductive physiology [McFarland et al., 1989]. LH/CG-R is a 7-transmembrane receptor found on testicular Leydig cells, and on ovarian theca, granulosa, luteal, and interstitial cells. The receptor is also found in the human uterus, placenta, umbilical cord, sperm and ovarian neoplasm. This receptor is also expressed in the lymphocytes from pregnant women and macrophages derived from term decidua [Katabuchi and Ohba, 2008]. In the chorionic villi of the human placenta, syncytiotrophoblasts and Hofbauer cells are positively immunostained with anti-human LH/CG-R antibody, which was raised against the exon 1-mapping extracellular domain of LH/CG-R of humans [Sonoda et al., 2005]. The present study showed that the cytoplasm of PMA-treated THP-1 cells was positively stained with this antibody.

In addition to the full-length LH/CG-R mRNA, multiple splicing variants of LH/CG-R mRNA are expressed that originate from a single gene encoding LH/CG-R in gonadal porcine, rat and human tissues [Loosfelt et al., 1989; Koo et al., 1994; Themmen and Huhtaniemi, 2000]. The human ovary and placenta express two forms of LH/CG-R mRNA, full-length LH/CG-R and LH/CG-R Δ9 [Minegishi et al., 1997]. Although these splicing variants of LH/CG-R seem to be conserved among mammalians, the physiological role of the gene products remains unknown. PMA-treated THP-1 cells express only an mRNA encoding LH/CG-R Δ9; however, it is unclear whether endogenous protein is synthesized from this mRNA. The present study revealed that PMA-treated THP-1 cells expressed only a 60-kDa protein designated as LH/CG-R Δ9. This molecular size was consistent with that of translated product expressed in mammalian 293 cells transfected with cDNA encoding human LH/CG-R Δ9; on the other hand, those transfected with cDNA of full-length LH/CG-R express two molecular bands of 85 kDa (mature band) and 68 kDa (immature band) [Nakamura et al., 2004]. This is the first report to demonstrate the endogenous production of the splicing variant of LH/CG-R protein.

Few reports have speculated on the function of human LH/CG-R Δ9. Rat LH/CG-R Δ9 is capable of binding hCG but is trapped in an intracellular compartment [Segaloff and Ascoli, 1993]. The extracellular domain of rat or human LH/CG-R without exon 9–11 has a high affinity for hCG because this domain shows a remarkable correspondence to leucine-rich repeats; therefore, human LH/CG-R Δ9 is thought to have high affinity for hCG [Ascoli et al., 2002]. The labeled human LH/CG-R Δ9 protein is not expressed on the cell surface in mammalian 293 cells [Nakamura et al., 2004]. The role of LH/CG-R Δ9 in human ovarian steroidogenic cells may be to control the function of full-length LH/CG-R in a dominant negative manner by forming heteromeric complexes with full-length LH/CG-R which acts as a signal transducer [Nakamura et al., 2004]; in contrast, the roles of LH/CG-R Δ9 in PMA-treated THP-1 cells must be different from those of LH/CG-R Δ9 coexpressed in human ovarian steroidogenic cells because PMA-treated THP-1 cells do not express the gene encoding the full-length LH/CG-R. We demonstrated that hCG induced a transient reduction in endogenous LH/CG-R Δ9 in PMA-treated THP-1 cells that was synchronous with the appearance of vacuoles. No such reduction in LH/CG-R Δ9 was induced by LH or FSH exposure, thus suggesting that LH and FSH cannot be incorporated into PMA-treated THP-1 cells and bound to cytoplasmic LH/CG-R Δ9. This hCG-induced transient reduction in LH/CG-R Δ9 led us to hypothesize that the intracellular

receptor with affinity for hCG recognizes hCG incorporated into the cytoplasm and transfers it to lysosomes for degradation, and LH/CG-R Δ9 may be subsequently replaced in the cytoplasm by protein synthesis. Moreover, human macrophages may represent cytoplasmic vacuoles mimicking the structure of Hofbauer cells while they are degrading hCG in lysosomes. In the present study, we did not investigate primary Hofbauer cells but PMA-treated THP-1 cells, a macrophage cell line. Hence, further studies on Hofbauer cells isolated from the chorionic villi are needed to elucidate the mechanism.

In conclusion, hCG temporarily induced both peculiar vacuole formation, morphologically mimicking Hofbauer cells and decreased expression of endogenous LH/CG-R Δ9 in human macrophages, which selectively incorporated hCG into the cytoplasm. Hofbauer cells may regulate hCG via cytoplasmic LH/CG-R Δ9 at the feto-maternal interface by the same mechanisms demonstrated in this study, and their characteristic vacuoles may be associated with the cell-specific function to protect the fetus from exposure to excess maternal hCG during pregnancy.

References

Ascoli, M., F. Fanelli, D.L. Segaloff (2002) The lutropin/choriogonadotropin receptor, a 2002 perspective. Endocr Rev *23:* 141–174.

Bradford, M.M. (1976) A rapid and sensitive method for the quantitation of microgram quantities of protein utilizing the principle of protein-dye binding. Anal Biochem *72:* 248–254.

Castellucci, M., P. Kaufmann (2006) Basic structure of the villous trees; in Kaufmann, P., R.N. Baergen (eds): Pathology of the Human Placenta. New York, Springer, vol 5, pp 50–120.

Clements, J.A., F.I. Reyes, J.S. Winter, C. Faiman (1976) Studies on human sexual development. III. Fetal pituitary and serum, and amniotic fluid concentrations of LH, CG, and FSH. J Clin Endocrinol Metab *42:* 9–19.

Cunningham, F.J., K.J. Leveno, J.C. Hauth, L.C. Gilstrap III, K.D. Wenstrom (2005) Implantation, embryogenesis, and placental development; in Rouse, D., B. Rainey, C. Spong, G.D. Wendel (eds): Williams Obstetrics. New York, McGraw-Hill, vol 22, pp 39–90.

Fox, H., N. Sebire (2007a) The development and structure of the placenta; in Houston, M., H. McCormick (eds): Pathology of the Placenta, Philadelphia, Saunders/Elsevier, vol 3, pp 17–56.

Fox, H., N. Sebire (2007b) Physiology of the placenta; in Houston, M., H. McCormick (eds): Pathology of the Placenta, Philadelphia, Saunders/Elsevier, vol 3, pp 57–67.

Frauli, M., H. Ludwig (1987) Demonstration of the ability of Hofbauer cells to phagocytose exogenous antibodies. Eur J Obstet Gynecol Reprod Biol *26:* 135–144.

Huhtaniemi, I.T., C.C. Korenbrot, R.B. Jaffe (1977) HCG binding and stimulation of testosterone biosynthesis in the human fetal testis. J Clin Endocrinol Metab *44:* 963–967.

Hume, D.A., I.L. Ross, S.R. Himes, R.T. Sasmon, Wells C.A., T. Ravasi (2002) The mononuclear phagocyte system revisited. J Leukoc Biol *72:* 621–627.

Ingman, K., V.J. Cookson, C.J. Jones, J.D. Aplin (2010) Characterisation of Hofbauer cells in first and second trimester placenta: incidence, phenotype, survival in vitro and motility. Placenta *31:* 535–544.

Katabuchi, H., M. Naito, S. Miyamura, K. Takahashi, H. Okamura (1989) Macrophages in human chorionic villi. Prog Clin Biol Res *296:* 453–458.

Katabuchi, H., Y. Fukumatsu, M. Araki, H. Mizutani, T. Ohba, H. Okamura (1994) Localization of chorionic gonadotropin in macrophages of the human chorionic villi. Endocr J *41(suppl):* S141–S153.

Katabuchi, H., T. Ohba (2008) Human chorionic villous macrophages as a fetal biological shield from maternal chorionic gonadotropin. Dev Growth Differ *50:* 299–306.

Khan, S., H. Katabuchi, M. Araki, T. Ohba, T. Koizumi, H. Okamura, R. Nishimura (2000) The molar vesicle fluid contains the beta-core fragment of human chorionic gonadotropin. Placenta *21:* 79–87.

Koo, Y.B., I. Ji, T.H. Ji (1994) Characterization of different sizes of rat luteinizing hormone/chorionic gonadotropin receptor messenger ribonucleic acids. Endocrinology *134:* 19–26.

Loosfelt, H., M. Misrahi, M. Atger, R. Salesse, M.T. Vu Hai-Luu Thi, A. Jolivet, A. Guiochon-Mantel, S. Sar, B. Jallal, J. Garnier, E. Milgrom (1989) Cloning and sequencing of porcine LH-hCG receptor cDNA: variants lacking transmembrane domain. Science *245:* 525–528.

Marc, A.F., S. Leon (2011) Hormone biosynthesis, metabolism, and mechanism of action; in Marc, A.F., S. Leon (eds) Clinical Gynecologic Endocrinology and Infertility, Baltimore, Lippincott Williams & Wilkins, vol 8, pp 29–104.

Matzuk, M.M., F.J. DeMayo, L.A. Hadsell, T.R. Kumar (2003) Overexpression of human chorionic gonadotropin causes multiple reproductive defects in transgenic mice. Biol Reprod *69:* 338–346.

McFarland, K.C., R. Sprengel, H.S. Phillips, M. Köhler, N. Rosemblit, K. Nikolics, D.L. Segaloff, P.H. Seeburg (1989) Lutropin-choriogonadotropin receptor: an unusual member of the G protein-coupled receptor family. Science *245:* 494–499.

Medeiros, de S.F., R.J. Norman (2009) Human choriogonadotrophin protein core and sugar branches heterogeneity: basic and clinical insights. Hum Reprod Update *15:* 69–95.

Minegishi, T., M. Tano, Y. Abe, K. Nakamura, Y. Ibuki, K. Miyamoto (1997) Expression of luteinizing hormone/human chorionic gonadotrophin (LH/HCG) receptor mRNA in the human ovary. Mol Hum Reprod *3:* 101–107.

Nakamura, K., S. Yamashita, Y. Omori, T. Minegishi (2004) A splice variant of the human luteinizing hormone (LH) receptor modulates the expression of wild-type human LH receptor. Mol Endocrinol *18:* 1461–1470.

Segaloff, D.L., M. Ascoli (1993) The lutropin/choriogonadotropin receptor... 4 years later. Endocr Rev *14:* 324–347.

Shi, Q.J., Z.M. Lei, C.V. Rao, J. Lin (1993) Novel role of human chorionic gonadotropin in differentiation of human cytotrophoblasts. Endocrinology *132:* 1387–1395.

Sonoda, N., H. Katabuchi, H. Tashiro, T. Ohba, R. Nishimura, T. Minegishi, H. Okamura (2005) Expression of variant luteinizing hormone/chorionic gonadotropin receptors and degradation of chorionic gonadotropin in human chorionic villous macrophages. Placenta *26:* 298–307.

Steinberg, D., J.L. Witztum (2010) Oxidized low-density lipoprotein and atherosclerosis. Arterioscler Thromb Vasc Biol *30:* 2311–2316.

Takasugi, N., T. Iguchi, J. Kurihara, A. Tei, M. Takase (1985) Changes in gonads of male and female offspring of mice receiving a continuous intravenous infusion of human chorionic gonadotropin during gestation. Exp Clin Endocrinol *86:* 273–283.

Themmen, A.P.N., I.T. Huhtaniemi (2000) Mutations of gonadotropins and gonadotropin receptors: elucidating the physiology and pathophysiology of pituitary-gonadal function. Endocr Rev *21:* 551–583.